

BIOLOGICAL CONTROL VIA “ECOLOGICAL” DAMPING: AN APPROACH THAT ATTENUATES NON-TARGET EFFECTS

Rana D. Parshad, Kelly Black, and Emmanuel Quansah

Department of Mathematics,
Clarkson University,
Potsdam, New York 13699, USA.

Matthew Beauregard

Department of Mathematics & Statistics,
Stephen F. Austin State University
Nacogdoches, TX, 75962, USA.

ABSTRACT. In this work we develop and analyze a mathematical model of biological control to prevent or attenuate the explosive increase of an invasive species population in a three-species food chain. We allow for finite time blow-up in the model as a mathematical construct to mimic the explosive increase in population, enabling the species to reach “disastrous” levels, in a finite time. We next propose various controls to drive down the invasive population growth and, in certain cases, eliminate blow-up. The controls avoid chemical treatments and/or natural enemy introduction, thus eliminating various non-target effects associated with such classical methods. We refer to these new controls as “ecological damping”, as their inclusion dampens the invasive species population growth. Further, we improve prior results on the regularity and Turing instability of the three-species model that were derived in [43]. Lastly, we confirm the existence of spatio-temporal chaos.

1. INTRODUCTION

Population dynamics are a fundamental aspect of many biological processes. In this paper, we introduce and investigate a mathematical model for the population dynamics of an invasive species in a three-species food chain model. Exotic species are defined as any species, capable of propagating themselves into a non-native environment. If the propagating species is able to establish a self sustained population in this new environment, it is formally defined as invasive. The survival and competitiveness of a species depends intrinsically on an individual’s fitness and ability to assimilate limited resources. Often invasive species possess the ability to dominate a particular resource. This allows them to expand their range via out-competing other native species. In the United States damages caused by invasive species to agriculture, forests, fisheries and businesses, have been estimated to be \$120 billion a year [47]. In the words of Daniel Simberloff: “*Invasive species are a greater threat to native biodiversity than pollution, harvest, and disease combined.*” [54] Therefore understanding and subsequently attenuating the spread of invasive species is an important and practical problem in spatial ecology and much work has

1991 *Mathematics Subject Classification.* Primary: 35K57,35B36,35B35,37D45; Secondary: 92D25,92D40.

Key words and phrases. Three-species food chain, finite time blow-up, spectral methods, global existence.

been devoted to this issue [1, 4, 10, 38, 40, 53]. More recently, the spread of natural and invasive species by nonrandom dispersal, say due to competitive pressures, is of great interest [2, 35]. However, there has been less focus, on the actual eradication of an invasive species, once it has already invaded. This is perhaps a harder problem. In the words of Mark Lewis: “*Once the invasive species are well established, there is not a lot you can do to control them*”. [66] It is needless to say however, that in many ecosystems around the world, invasion has already taken place! Some prominent examples in the US, are the invasion by the Burmese python in southern regions of the United States, with climatic factors supporting their spread to a third of the United States [50]. The sea lamprey and round goby have invaded the Great Lakes region in the northern United States and Canada [7]. These species have caused a severe decline in lake trout and other indigenous fish populations. Lastly the Zebra Mussel has invaded many US and Canadian waterways causing large scale losses to the hydropower industry [39].

Another factor attributed to the increase of an invasive population, is that the environment may turn favorable for the invasive species in question, while becoming unfavorable for its competitors or natural enemies. In such situations, the population of the invasive species may rapidly increase. This is defined as an *outbreak* in population dynamics [6]. These rapid changes tend to destabilize an ecosystem and pose a threat to the natural environment. As an illustration, in the European Alps certain environmental conditions have enabled the population of the larch budmoth to become large enough that entire forests have become defoliated [36]. In most ecological landscapes, due to exogenous factors, one always encounters an invasive species and an invaded species. If the density of the former, be it invasive, disease causing, an agricultural pest, defoliator or other, undergoes a rapid transition to a high level in population, the results can be catastrophic both for local and nonlocal populations.

Biological and chemical controls are an adopted strategy to limit invasive populations [65]. Chemical controls are most often based on direct methods, via the use of pesticides [65]. Biological control comprises of essentially releasing natural enemies of the invasive species/pest against it. These can be in the form of predators, parasitoids, pathogens or combinations thereof [65]. There are many problems with these approaches. For example, a local eradication effort was made by USGS through a mass scale poisoning of fish in order to prevent the asian carp (an invasive fish species) from entering the Chicago Sanitary and Ship Canal [30]. The hope was to protect the fishing interests of the region. However, among the tens of thousands of dead fish, *biologists found only one asian carp*. Thus chemical control is not an exhaustive strategy. However, biological controls are also not without its share of problems. In fact, sometimes the introduced species might attack a variety of species, other than those it was released to control. This phenomena is referred to as a *non-target effect* [16, 34], and is common in natural enemies with a broad host range. For example, the cane toad was introduced in Australia in 1935 to control the cane beetle. However, the toad seemingly attacked everything else but its primary target [46]! In addition, the toad is highly poisonous and therefore predators shy away from eating it. This has enabled the toad population to grow virtually unchecked and is today considered one of Australia’s worst invasive species [55]. In studies of biological control in the United States estimate that when parasitoids are released as biological controls that 16% of the introduced species

will attack non-targets, in Canada these numbers are estimated as high as 37.5% [16]. In practise it is quite difficult to accurately predict these numbers. The current drawbacks make it clear that alternative controls are necessary. Furthermore, that modeling of alternative controls is important to validate the effectiveness of a management strategy that hopes to avoid non-target effects. Such modeling is essential to access and predict the best controls to employ, so that the harmful population will decrease to low and manageable levels. This then gives us confidence to devise actual field trials. We should note that in practice actual eradication is rarely achieved.

Thus there are clear questions that motivate this research:

- (1) How does one define a “high” level for a population, and further, how well does an introduced control actually work, at various high levels?
- (2) Is it possible to design controls that avoid chemicals/pesticides/natural enemy introduction, and are still successful?

This paper addresses these questions through the investigation of a mathematical model that:

- (1) Blows-up in finite time. Given a mathematical model for a nonlinear process, say through a partial differential equation (PDE), one says finite time blow up occurs if

$$\lim_{t \rightarrow T^* < \infty} \|r\|_X \rightarrow \infty,$$

where X is a certain function space with a norm $\|\cdot\|$, r is the solution to the PDE in question, and T^* is the blow up time. Therefore “highest” level is equated with blow up, and the population passes through every conceivable high level of population as it approaches infinity.

- (2) Incorporates certain controls that avoid chemicals/pesticides/natural enemy introduction. The controls we examine are:
 - (a) The primary food source of the invasive species is protected through spatial refuges. The regions that offer protection are called *prey refuges* and may be the result of human intervention or natural byproducts, such as improved camouflage.
 - (b) An overcrowding term is introduced to model the movement or dispersion from high concentrations of the invasive species. Densely populated regions have increased intraspecific competition and interference which cause an increase in the dispersal of the invasive species. This is an improvement to current mathematical models and will be seen to be beneficial if used a control.
 - (c) We introduce role reversing mechanisms, where the role of the primary food source of the invasive species, and the prey of this food source, is switched in the open area (the area without refuge). This models situations where the topography provides competitive advantages to certain species. It will be seen that this also is beneficial if used a control. In effect, this uses the current ecosystem and by modifying the landscape a natural predator in the environment has an advantage in key areas. Hence, the invasive species population will adversely be effected. It can also be thought of as introducing a competitor of the invasive species, to compete with it for its prey.

Remark 1. Note, none of the above rely on enemy release to predate on the invasive species, or a parasite or pathogen release to infect the invasive species. Thus potential non-target effects due to such release can be avoided.

In the literature finite time blow up is also referred to as an explosive instability [58]. There is a rich history of blow up problems in PDE theory and its interpretations in physical phenomenon. For example, this feature is seen in models of thermal runaway, fracture and shock formation, and combustion processes. Thus blow up may be interpreted as the failure of certain constitutive materials leading to gradient catastrophe or fracture, it may be interpreted as an uncontrolled feedback loop such as in thermal runaway, leading to explosion. It might also be interpreted as a sudden change in physical quantities such as pressure or temperature such as during a shock or in the ignition process. The interested reader is referred to [48, 58]. Blow up in population dynamics is usually interpreted as excessively high concentrations in small regions of space, such as seen in chemotaxis problems [26]. Our goal in the current manuscript is to bring yet another interpretation of blow up to population dynamics, that is one where we equate such an excessive concentration or “blow up” of an invasive population with disaster for the ecosystem. Furthermore, it is to devise controls that avoid non-target effects and yet reduce the invasive population, before the critical blow up time.

In the following, the norms in the spaces $\mathbb{L}^p(\Omega)$, $\mathbb{L}^\infty(\Omega)$ and $\mathbb{C}(\overline{\Omega})$ are respectively denoted by

$$\|u\|_p^p = \frac{1}{|\Omega|} \int_{\Omega} |u(x)|^p dx, \quad \|u\|_\infty = \max_{x \in \Omega} |u(x)|.$$

In addition, the constants C , C_1 and C_2 may change between subsequent lines, as the analysis permits, and even in the same line if so required.

The current manuscript is organised as follows. In section 2 we formulate the spatially explicit model that we consider. In section 3 we describe in detail the modeling of the control mechanisms that we propose, and term “ecological damping”. Here we make three key conjectures 1, 2 and 3, concerning our control mechanisms. Section 4 is devoted to some analytical results given via lemma 4.3, theorem 4.4 and 4.5. Section 5 is where we explain our numerical approximations and test conjectures 1, 2 and 3 numerically. In section 6 we investigate spatio-temporal dynamics in the model. We investigate the effect of overcrowding on Turing patterns, and we also confirm spatio-temporal chaos in the model. Lastly we offer some concluding remarks and discuss future directions in section 7.

2. MODEL FORMULATION

A three species food chain model is developed, where the top predator, denoted as r , is invasive. In our model, r may blow up in finite time. Although populations cannot reach infinite values in finite time, they can grow rapidly [6]. The blow up event indicates that the invasive population has reached “an extremely high” and uncontrollable level. Naturally, that level occurs prior to the blow up time. Therefore, as $\|r\|$ approaches infinity in finite time, it passes through every conceivable “high” level. The blow up time, T^* , is viewed as the “disaster” time. We investigate mechanisms that attempt to lower and control the targeted population *before time T^** . This modeling approach has distinct advantages:

- (1) There is no ambiguity as to what is a disastrous high level of population.
- (2) There is a clear demarcation between when or if the disaster occurs.
- (3) The controls that are proposed do not rely on a direct attack on the invasive species, as is the traditional approach, rather we attempt to control the food source of r . This will avoid possible nontarget effects.
- (4) The model provides a useful predictive tool that can be tuned and established through data, in various ecological settings.
- (5) Mathematical models are advantageous in many situations due to their cost-effectiveness and versatility. Of course obtaining an analytical solution for a nonlinear model is virtually impossible, outside of special cases. However, a numerical approximation can be developed to accurately investigate the role and effect our controls have on the blow up behavior.

Suppose an invasive species r has invaded a certain habitat and it has become the top predator in a three species food chain. Hence, r predaes on a middle predator v , which in turn predaes on a prey u . A temporal model is given for the species interaction, namely

$$\begin{aligned}
 (1) \quad \frac{dr}{dt} &= cr^2 - w_3 \frac{r^2}{v + D_3}, \\
 (2) \quad \frac{dv}{dt} &= -a_2v + w_1 \left(\frac{uv}{u + D_1} \right) - w_2 \left(\frac{vr}{v + D_2} \right), \\
 (3) \quad \frac{du}{dt} &= a_1u - b_2u^2 - w_0 \left(\frac{uv}{u + D_0} \right).
 \end{aligned}$$

The spatial dependence is included via diffusion,

$$\begin{aligned}
 (4) \quad \partial_t r &= d_3 \Delta r + cr^2 - w_3 \frac{r^2}{v + D_3} = h(u, v, r), \\
 (5) \quad \partial_t v &= d_2 \Delta v - a_2v + w_1 \frac{uv}{u + D_1} - w_2 \frac{vr}{v + D_2} = g(u, v, r), \\
 (6) \quad \partial_t u &= d_1 \Delta u + a_1u - b_2u^2 - w_0 \frac{uv}{u + D_0} = f(u, v, r),
 \end{aligned}$$

defined on $\mathbb{R}^+ \times \Omega$. Here $\Omega \subset \mathbb{R}^N$, $N = 1, 2$ and Δ is the one or two dimensional Laplacian operator. We define \mathbf{x} to be the spatial coordinate vector in one or two dimensions. The parameters d_1 , d_2 and d_3 are positive diffusion coefficients. Neumann boundary conditions are specified on the boundary. The initial populations are given as

$$u(0, \mathbf{x}) = u_0(\mathbf{x}), v(0, \mathbf{x}) = v_0(\mathbf{x}), r(0, \mathbf{x}) = r_0(\mathbf{x}) \quad \text{in } \Omega,$$

are assumed to be nonnegative and uniformly bounded on Ω .

There are various parameters in the model: a_1 , a_2 , b_2 , w_0 , w_1 , w_2 , w_3 , c , D_0 , D_1 , D_2 , and D_3 are all positive constants. Their definitions are as follows: a_1 is the growth rate of prey u ; a_2 measures the rate at which v dies out when there is no u to prey on and no r ; w_i is the maximum value that the per-capita rate can attain; D_0 and D_1 measure the level of protection provided by the environment to the prey; b_2 is a measure of the competition among prey, u ; D_2 is the value of v at which its per capita removal rate becomes $w_2/2$; D_3 represents the loss in r due to the lack of its favorite food, v ; c describes the growth rate of r via sexual reproduction.

These models offer rich dynamics and were originally proposed in [60, 61] in order to explain why chaos has rarely been observed in natural populations of three interacting species. The model stems from the Leslie-Gower formulation and considers interactions between a generalist top predator, specialist middle predator and prey. The study of these models have generated much research [18, 32, 33, 41, 43, 62, 63, 64]. An interesting fact is if $c > \frac{w_3}{D_3}$ the spatially independent and spatially dependent models are easily seen to blow up in finite time [42]. The spatially dependent model offers further rich dynamics, in particular the possibility of Turing instabilities and non Turing patterns [32, 43]. Nevertheless, to avoid blow up it appears that one must restrict $c < K \frac{w_3}{D_3}$, where $K < 1$. This was established for the spatially independent model in [3] and is offered here for convenience:

Theorem 2.1. *Consider the model (1)-(3). Under the assumption that*

$$(7) \quad c < \left(\frac{w_0 b_2 D_3}{w_1 \left(a_1 + \frac{a^2}{4a_2} \right) + w_0 b_2 D_3} \right) \frac{w_3}{D_3},$$

all non-negative solutions (i.e. solutions initiating in \mathbb{R}_+^3) of (1)-(3) are uniformly bounded forward in time and they eventually enter an attracting set \mathcal{A} .

Remark 2. We have recently shown the above result to be *false* in the ODE and PDE cases. That is, (4)-(6) may blow up in finite time, even under (7) provided the initial data is large enough [44]. It is clear that even if (7) is maintained r can blow up. This becomes more evident if we consider the coefficient $c - \frac{w_3}{v+D_3}$ on r^2 and the fact that if the fecundity of r is large compared to $\frac{w_3}{v+D_3}$ then blow up will occur. This may happen in situations where:

- (1) There is an abundance of v ,
- (2) r possesses certain abilities to out compete other species, and harvest enough v ,
- (3) The environment has turned favorable for r and unfavorable for its natural enemies or competitors. Thus it can harvest v unchecked.

Remark 3. If no intervention is made we can envision r growing to disastrous levels with adequate initial resources. The blow up time T^* is viewed as the point of disaster in an ecosystem. Thus one is interested in controlling r via the use of biological controls, before the critical time T^* .

Remark 4. These observations motivate an interesting question. Assume that both (1)-(3) and its spatially explicit form (4)-(6) blow up in finite time for $c < \frac{w_3}{D_3}$ for a given initial condition. Can we modify (4)-(6), via introducing certain controls, so that now *there is no blow up*, for the same initial condition?

3. DELAY AND REMOVAL OF BLOW UP VIA “ECOLOGICAL DAMPING”

It is clear that controlling the population of an invasive specie is advantageous, and most often necessary. However the avenues for which this is possible, whilst avoiding non-target effects, is not clear. Here, we propose new controls that may delay or even remove blow-up in the invasive population. We refer to these controls as “ecological damping”, akin to damping forces such as friction in physical systems, that add stability to a system. The crux of our idea is to use prey refuges, in conjunction with role reversal and overcrowding effects. There is a vast literature on

prey refuge, spatial refuges as well as role reversal in the literature. The interested reader is referred to [12, 15, 29]. However, to the best of our knowledge these have not been proposed as control mechanisms for invasive species.

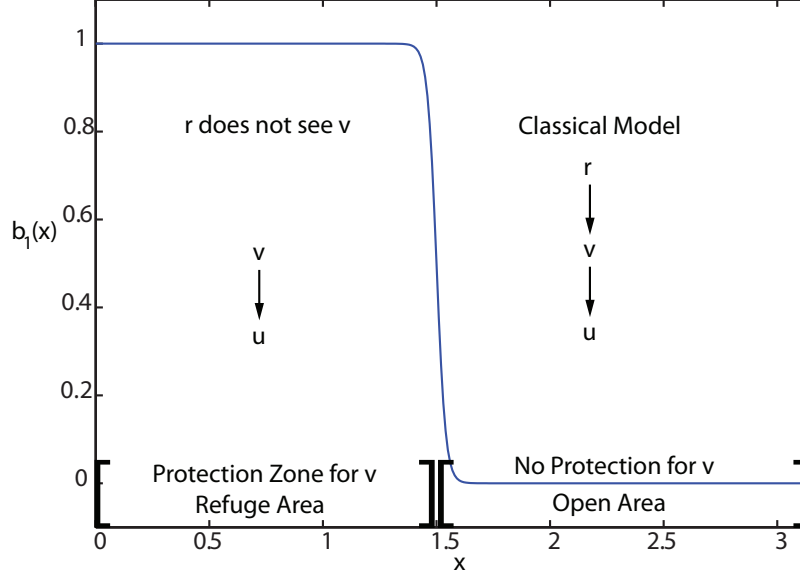


FIGURE 1. An example of a prey refuge function $b_1(x) = \frac{1}{2} (1 - \tanh(\frac{x-a}{\epsilon}))$ in the one dimensional case. This function decreases monotonically throughout its domain. The range is $0 \leq b_1(x) \leq 1$. If $b_1(x) = 1$ then the prey v is protected while if $b_1(x) = 0$ then v is unprotected.

3.1. Prey Refuge: Modified Model I. We consider modeling a prey refuge. Consider the continuous function $b_1(\mathbf{x})$. The region where $b_1(\mathbf{x}) = 1$ or sufficiently close to one is defined as a *prey refuge domain* or *patch*. We call the region where $b_1(\mathbf{x}) = 0$ or sufficiently close to zero an open area, this is the region where r can predate on v . In Figure 1 we see a sharp gradient between the prey refuge domain and the open area.

The inclusion of a prey refuge influences the equations for r and v , namely,

$$(8) \quad r_t = d_3 \Delta r + cr^2 - w_3 \frac{r^2}{(1 - b_1)v + D_3}$$

$$(9) \quad v_t = d_2 \Delta v - a_2 v + w_1 \left(\frac{uv}{u + D_1} \right) - w_2 (1 - b_1) \left(\frac{vr}{v + D_2} \right),$$

posed on a bounded domain in one or two dimensions. Neumann boundary conditions are specified. The equation for u may be found in (6).

The introduction of the prey refuge creates regions where it is impossible for r to predate on v . Notice, that if the entire spatial domain is considered a prey refuge, that is, $b_1(\mathbf{x}) = 1 \forall \mathbf{x} \in \Omega$, then the coefficient of r^2 will depend on the sign of $c < \frac{w_3}{D_3}$. If this is negative, then the invasive species dies off. Likewise, in

the absence of a prey refuge, that is, $b_1(\mathbf{x}) = 0 \forall \mathbf{x} \in \Omega$ the equations for r and v collapse to our previous ones, that is, (4) and (5), respectively. In such a case, it is known that blow up may still occur for sufficiently large enough data even if $c < \frac{w_3}{D_3}$. This is because the coefficient of r^2 may still be positive, as one always has $\frac{w_3}{v+D_3} < c < \frac{w_3}{D_3}$. The introduction of the refuge *forces* the coefficient of r^2 to change sign between the refuge and the open area. In the literature such problems are referred to as indefinite parabolic problems. The word *indefinite* refers to the sign of the coefficient being indefinite. Although there is a vast literature on such problems for single species models [19, 49], there is far less work for systems. There is also a large amount of literature for such switching mechanisms incorporated to understand competitive systems [20, 21], particularly in the vein of human economic progress.

This indefinite parabolic problem motivates a collection of questions: If blow up occurs for particular parameters in the case $b_1(\mathbf{x}) = 0$, will a prey refuge prevent blow up? How does this depend on the geometry of the refuge? What is the critical size or shape of a refuge that prevents blow up from occurring? Does this depend on the size of the initial condition? In the situation that blow up still persists, how is the blow up time affected? Are these results influenced by multiple refuges?

In either case, we make the conjecture:

Conjecture 1. *Consider the three species food chain model (4)-(6), a set of parameters with $c < \frac{w_3}{D_3}$, and an initial condition (u_0, v_0, r_0) such that r which is the solution to (4), blows up in finite time, that is*

$$\lim_{t \rightarrow T^* < \infty} \int_{\Omega} r(\mathbf{x}, t) d\mathbf{x} \rightarrow \infty,$$

there exists a patch $\Omega_1 \subset \Omega$, s.t for any single patch of measure greater than or equal to $|\Omega_1|$, the modified model (8)-(9), with the same parameter set and initial condition, has globally existing solutions. In particular the solution r to (8), does not blow up in finite time.

Proof. A proof of this conjecture can be established for certain special cases in one dimension. Assume (4)-(6) blows up at time $t = T^*$, for a certain parameter set and an initial condition $r_0(x)$, such that $r_0(\pi) = 0$. We consider now introducing a refuge at the right end, starting at some positive $a < \pi$. Now for $x \in [a, \pi]$ the density of v decreases, and the coefficient of r^2 is $\left(c - \frac{w_3}{D_3}\right) < 0$, hence r is restricted on the right hand side of the domain. We assume that this is equivalent to introducing a Dirichlet boundary condition somewhere in the closed interval $[a, \pi]$. Thus the modified model is equivalent to

$$(10) \quad r_t = d_3 \Delta r + cr^2 - w_3 \frac{r^2}{v + D_3}, \text{ on } [0, b], \text{ where } a < b < \pi,$$

and $r_x(0, t) = 0$ and $r(b, t) = 0$. Here we assume the initial condition satisfies $r_0(b) = 0$. Let us now compare (10) to

$$(11) \quad r_t = d_3 \Delta r + cr^2, \text{ on } [0, b], \text{ where } a < b < \pi.$$

The solution of the above is a supersolution to (10). However we know that there exists small data solutions to (11). This is easily seen via following the methods in [68]. Basically without loss of generality we may assume $c = d_3 = 1$. We then

multiply (11) by r_t and integrate by parts in $(0, b)$ to obtain

$$\frac{d}{dt} \left(\frac{1}{2} \|r_x\|_2^2 - \frac{1}{3} \|r\|_3^3 \right) + \|r_t\|_2^2 = 0,$$

thus

$$\frac{d}{dt} \left\{ \|r_x\|_2^2 - \frac{2}{3} \|r\|_3^3 \right\} \leq 0,$$

We now define the functional

$$E(t) = \|r_x(t)\|_2^2 - \frac{2}{3} \|r(t)\|_3^3,$$

Since $E'(t) \leq 0$ we obtain

$$E(t) \leq E(0) = \|\partial_x r_0\|_2^2 - \frac{2}{3} \|r_0\|_3^3.$$

Now we multiply (11) by r and integrate by parts in $(0, b)$ to obtain

$$(12) \quad \frac{1}{2} \frac{d}{dt} \|r\|_2^2 + \|r_x\|_2^2 - \|r\|_3^3 = 0.$$

This yields

$$(13) \quad \frac{1}{2} \frac{d}{dt} \|r\|_2^2 + E - \frac{1}{3} \|r\|_3^3 = 0.$$

So If $E(0) < 0$, then $E(t) < E(0) < 0$ and so

$$(14) \quad \frac{1}{2} \frac{d}{dt} \|r\|_2^2 \geq \frac{1}{3} \|r\|_3^3.$$

This essentially yields

$$(15) \quad \frac{d}{dt} \|r\|_2^2 \geq \frac{2}{3} (\|r\|_2^2)^{\frac{3}{2}}.$$

Setting $Y(t) := \|r(t)\|_2^2$. We derive the following differential inequality $Y' \geq \frac{2}{3} Y^{3/2}$. and so

$$\|r(t)\|_2^2 \geq \frac{3\|r_0\|_2^2}{3-t\|r_0\|_2^2}.$$

which means the solutions exist for $t \in [0, T^*)$, where

$$(16) \quad T^* = \frac{3}{\|r_0\|_2^2}, \quad r_0 \neq 0.$$

and then the solution r blows up at time T^* . This means that if $E(0) \geq 0$, then the initial data is actually small enough to ensure globally existing solutions [68]. What is required is

$$(17) \quad \|\partial_x r_0\|_2^2 \geq \frac{2}{3} \|r_0\|_3^3.$$

This criteria can always be obtained for large enough refuge, that is, for b small enough. Since the boundary terms cancel, the norm here is equivalent to the $H_0^1(0, b)$ norm, hence by Sobolev embedding we have

$$(18) \quad \int_0^b |\partial_x r_0|^2 dx \geq C \left(\int_0^b |r_0|^3 dx \right)^{\frac{2}{3}}$$

Now since $\int_0^b |r_0|^3 dx \ll 1$, for b chosen small enough we obtain

$$(19) \quad C \left(\int_0^b |r_0|^3 dx \right)^{\frac{2}{3}} > \frac{2}{3} \left(\int_0^b |r_0|^3 dx \right)$$

Thus combining (18) and (19) we obtain

$$(20) \quad \int_0^b |\partial_x r_0|^2 dx \geq C \left(\int_0^b |r_0|^3 dx \right)^{\frac{2}{3}} > \frac{2}{3} \left(\int_0^b |r_0|^3 dx \right).$$

This proves a particular case of conjecture 1. \square

3.2. The Overcrowding Effect: Modified Model II. In high population density areas a species should have greater dispersal in order to better assimilate available resources and avoid crowding effects such as increased intraspecific competition. These effects can be modeled via an overcrowding term, that has not been included in mathematical models of biological control. Consider the improved mathematical model that includes an overcrowding effect of the invasive species r , namely,

$$(21) \quad r_t = d_3 r_{xx} + cr^2 - w_3 \frac{r^2}{v + D_3} + d_4 (r^2)_{xx},$$

$$(22) \quad v_t = d_2 v_{xx} - a_2 v + w_1 \left(\frac{uv}{u + D_1} \right) - w_2 \left(\frac{vr}{v + D_2} \right),$$

with initial and boundary conditions as before. Again, the equation for u remains unchanged. The addition of $d_4 (r^2)_{xx} \equiv \frac{d_4}{2} (rr_{xx})_x$ represents a severe penalty on local overcrowding. This is interpreted as movement from high towards low concentrations of r , directly proportional to r . Hence, r attempts to avoid overcrowding and disperses toward lower concentrations. Such models have been under intense investigation recently and are referred to as cross-diffusion and self-diffusion systems [53]. The mathematical analysis of such models is notoriously difficult [27, 28]. We limit ourselves to the one-dimensional case in the forthcoming analysis and its numerical approximations. Therefore the one dimensional Laplacian is considered in (6).

The presence of blow up is not affected if we maintain Neumann boundary conditions at the boundaries. This can be seen in a straightforward manner. Let us assume the classical model, that is (4)-(6), blows up. Therefore, without loss of generality, there exists a δ such that $\left(c - \frac{w_3}{v + D_3} \right) > \delta > 0$. This implies that if we set $H(t) = \int_{\Omega} r(x, t) dx$, then,

$$\frac{d}{dt} H(t) \geq \frac{\delta}{\sqrt{|\Omega|}} H(t)^2,$$

leading to the blow up of $H(t)$. Now, consider the integration over Ω of (21). Since the overcrowding term integrates to zero then blow up still persists. However, a combination of a prey refuge with the overcrowding effect may prevent blow up. Further, we expect it takes a smaller refuge to accomplish the removal of blow up. This is precisely the following conjecture:

Conjecture 2. Consider the three species food chain model (4)-(6), a set of parameters, such that $c < \frac{w_3}{D_3}$, and an initial condition (u_0, v_0, r_0) such that r which is the solution to (4), blows up in finite time, that is

$$\lim_{t \rightarrow T^* < \infty} \int_{\Omega} r(\mathbf{x}, t) d\mathbf{x} \rightarrow \infty, \quad T^* < \infty,$$

there exists a patch $\Omega_2 \subset \Omega$, and an overcrowding coefficient d_4 , s.t for any single patch of measure greater than or equal to $|\Omega_2|$, the modified model (21)-(22), with the same parameter set and initial condition, has globally existing solutions. In particular The solution r to (21), does not blow up in finite time. Furthermore, $\Omega_2 \subset \Omega_1$, where Ω_1 is the patch found in conjecture (1).

This is not difficult to see, as multiplying through by r and integrating by parts yields

$$\frac{1}{2} \frac{d}{dt} \|r\|_2^2 + E - \frac{1}{3} \|r\|_3^3 + \int_{\Omega} r |r_x|^2 dx = 0.$$

So If $E(0) < 0$, then $E(t) < E(0) < 0$ and so

$$(23) \quad \frac{1}{2} \frac{d}{dt} \|r\|_2^2 + \int_{\Omega} r |r_x|^2 dx \geq \frac{1}{3} \|r\|_3^3 > \frac{2}{3} (\|r\|_2^2)^{\frac{3}{2}}.$$

Thus even if one has negative energy, $E(t) \leq E(0) < 0$ so that (8) blows-up, due to the presence of the positive $\int_{\Omega} r |r_x|^2 dx$ term in (23), (21) will not blow up for small data, thus yielding a global solution. Thus there are initial data for which (8) blow ups but (21) does not, and so a smaller refuge would work in this case. The method follows by mimicing the steps in (12)-(20), with the additional $\int_{\Omega} r |r_x|^2 dx$ term.

3.3. Refuge, Overcrowding, and Role Reversal: Modified Model III. The prey refuge and overcrowding are included in the one-dimensional mathematical model. We also include a role-reversal of u within the protection zone of the refuge. This models the scenario in which two species may prey on each other in various regions where it is advantageous. Hence, the role-reversal of u will compete with the invasive species r . Figure 2 depicts the scenario of a one dimensional prey refuge for which outside the protection zone both u and r may predate on v . Hence, the model we propose of this scenario is given below,

$$(24) \quad r_t = d_3 r_{xx} + \left(c - \frac{w_3}{(1 - b_1(x))v + D_3}\right) r^2 + d_4 (r^2)_{xx},$$

$$v_t = d_2 v_{xx} - a_2 v + b_1(x) w_1 \frac{uv}{u + D_1}$$

$$(25) \quad -(1 - b_1(x)) \left(w_4 \frac{vu}{v + D_2} + w_2 \frac{vr}{v + D_4} \right),$$

$$(26) \quad u_t = d_1 u_{xx} + a_1 u - b_2 u^2 + (1 - b_1(x)) w_5 \frac{vu}{v + D_0} - b_1(x) w_1 \frac{uv}{u + D_3}.$$

In light of this model we propose Conjecture 3:

Conjecture 3. Consider the three species food chain model (4)-(6), a set of parameters such that $c < \frac{w_3}{D_3}$, and an initial condition (u_0, v_0, r_0) such that r which is the solution to (4), blows up in finite time, that is

$$\lim_{t \rightarrow T^* < \infty} \int_{\Omega} r(\mathbf{x}, t) d\mathbf{x} \rightarrow \infty, \quad T^* < \infty,$$

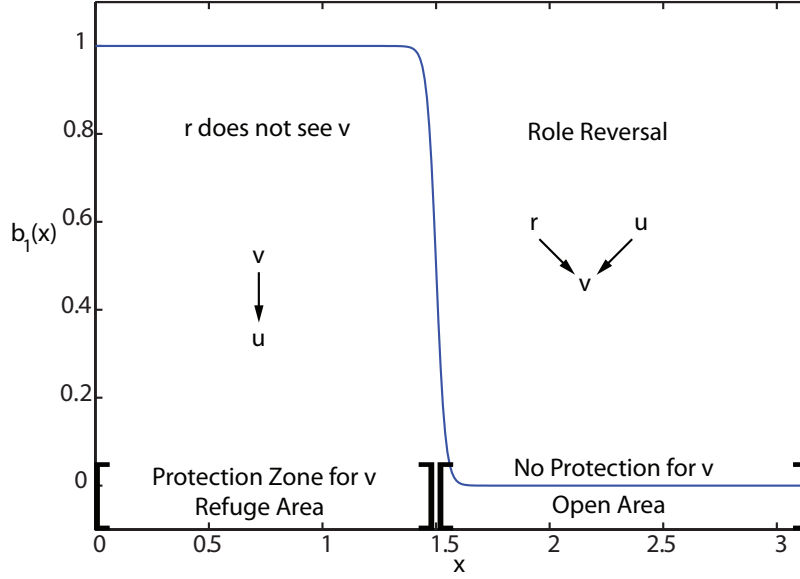


FIGURE 2. This shows a plot of the refuge function $b_1(x) = \frac{1}{2} (1 - \tanh(\frac{x-a}{\epsilon}))$. In certain regions u has a disadvantage over v , while outside of this u is able to prey on v . The invasive species effect on v is influenced by the prey refuge.

there exists a patch $\Omega_3 \subset \Omega$ such that the modified model (24)-(26), with the same parameter set and initial condition, has globally existing solutions. In particular, the solution r to (24) does not blow up in finite time. Furthermore, $\Omega_3 \subset \Omega_2$, where Ω_2 is the patch found in conjecture (2).

All three conjectures are tested numerically in Section 5.3.

4. FORMAL ESTIMATES AND REGULARITY

4.1. Preliminaries. The nonnegativity of the solutions of (4)-(6) is preserved by application of standard results on invariant regions [57]. This is due to the reaction terms being quasi-positive, that is,

$$f(0, v, r) \geq 0, \quad g(u, 0, r) \geq 0, \quad h(u, v, 0) \geq 0, \quad \text{for all } u, v, r \geq 0.$$

Since the reaction terms are continuously differentiable on \mathbb{R}^3 , then for any initial data in $\mathbb{C}(\overline{\Omega})$ or $\mathbb{L}^p(\Omega)$, $p \in (1, +\infty)$, it is easy to directly check their Lipschitz continuity on bounded subsets of the domain of a fractional power of the operator $I_3(d_1, d_2, d_3)^t \Delta$, where I_3 the three dimensional identity matrix, Δ is the Laplacian operator and $()^t$ denotes the transposition. Under these assumptions, the following local existence result is well known (see [17, 24, 45, 51, 57]).

Proposition 1. *The system (4)-(6) admits a unique, classical solution (u, v, r) on $[0, T_{\max}[\times \Omega$. If $T_{\max} < \infty$ then*

$$\lim_{t \nearrow T_{\max}} \{ \|u(t, \cdot)\|_{\infty} + \|v(t, \cdot)\|_{\infty} + \|r(t, \cdot)\|_{\infty} \} = \infty.$$

Lemma 4.1 (Uniform Gronwall Lemma). *Let β , ζ , and h be nonnegative functions in $L^1_{loc}[0, \infty; \mathbb{R})$. Assume that β is absolutely continuous on $(0, \infty)$ and the following differential inequality is satisfied:*

$$\frac{d\beta}{dt} \leq \zeta\beta + h, \text{ for } t > 0.$$

If there exists a finite time $t_1 > 0$ and some $q > 0$ such that

$$\int_t^{t+q} \zeta(\tau) d\tau \leq A, \int_t^{t+q} \beta(\tau) d\tau \leq B, \text{ and } \int_t^{t+q} h(\tau) d\tau \leq C,$$

for any $t > t_1$, where A, B , and C are some positive constants, then

$$\beta(t) \leq \left(\frac{B}{q} + C \right) e^A, \text{ for any } t > t_1 + q.$$

4.2. Improvement of Regularity of the Classical Model.

4.2.1. Improvement of the Global Existence Condition. In this section we improve the global existence conditions that has been derived recently in [43]. Here, we provide the previous result, Theorem 4.2.

Theorem 4.2. *Consider the three-species food-chain model described by (4)-(6). For any initial data $(u_0, v_0, r_0) \in L^2(\Omega)$, such that $\|v_0\|_\infty \leq \frac{w_3}{c} - D_3$, and parameters (c, w_3, D_3) such that $\|v\|_\infty \leq \frac{w_3}{c} - D_3$, there exists a global classical solution (u, v, r) to the system.*

We now give an improved result for the ODE case, which is easily modified for PDE case. In essence, given any initial data (however large), there is global solution, for a_2 appropriately large. This is summarised in following lemma,

Lemma 4.3. *Consider the three-species food-chain model described by (1)-(3). As long as $c < \frac{w_3}{D_3}$, given any initial data (u_0, v_0, r_0) , however large, there exists a global solution (u, v, r) to the system as long as the parameter a_2 is s.t*

$$a_2 \geq w_1 + c|r_0| \ln \left(\frac{|v_0|}{w_3/c - D_3} \right),$$

Proof. Consider the following subsystem

$$(27) \quad \frac{dv}{dt} = -a_2 v + w_1 v,$$

$$(28) \quad \frac{dr}{dt} = cr^2.$$

The v here grows faster than the v determined by (2). Similarly, the r here blows up faster than r in (1). In order to drive v down below $w_3/c - D_3$, we use the exact solution to (27), that is,

$$v = e^{-(a_2 - w_1)t} v_0$$

Assuming that $a_2 > w_1$, then for v to be below $w_3/c - D_3$ implies that

$$e^{-(a_2 - w_1)t} v_0 \leq w_3/c - D_3$$

Thus when $t > T^* = \frac{1}{a_2 - w_1} \ln \left(\frac{|v_0|}{w_3/c - D_3} \right)$, we shall have

$$e^{-(a_2 - w_1)t} v_0 = v \leq w_3/c - D_3.$$

Now (28) blows up at time $T^{**} = \frac{1}{c|r_0|}$. So if we choose a_2 appropriately, we can make $T^* < T^{**} = \frac{1}{c|r_0|}$. This is done by choosing

$$\frac{1}{a_2 - w_1} \ln \left(\frac{|v_0|}{w_3/c - D_3} \right) = T^* < T^{**} = \frac{1}{c|r_0|}$$

Thus if a_2 is s.t $a_2 \geq w_1 + c|r_0| \ln \left(\frac{|v_0|}{w_3/c - D_3} \right)$, then $v \leq w_3/c - D_3$, before r blows up. Therefore, if we consider the r determined by (1) then this will certainly not blown up by time $t = T^*$. At this point however, $c - \frac{w_3}{v+D_3}$ is negative, so r in (1), cannot blow up after T^* , and will decay. In this latter case the global attractor is a very simple, $(u, v, r) = (u^*, v^*, 0)$. Hence, we have an extinction state for r .

In short, we see that for any initial condition that is specified, there exists an a_2 (depending on the initial condition), s.t (1)-(3) has a global solution. \square

4.2.2. Uniform $L^2(\Omega)$ and $H^1(\Omega)$ Estimates. We recap the following estimate from [42]

$$\|u\|_2^2 \leq e^{-\frac{b_1}{C_1}t} \|u(0)\|_2^2 + \frac{CC_1}{b_1}.$$

Therefore, there exists time t_1 given explicitly by

$$t_1 = \max \left\{ 0, C_1 \frac{\ln(\|u(0)\|_2^2)}{b_1} \right\},$$

such that, for all $t \geq t_1$, the following estimate holds uniformly:

$$\|u\|_2^2 \leq 1 + \frac{CC_1}{b_1}.$$

Here t_1 is the compactification time of $\|u\|_2$.

We also recall the following local in time integral estimate for ∇u , from [42]

$$\int_t^{t+1} \|\nabla u\|_2^2 ds \leq \frac{1}{2d_1} \|u(t)\|_2^2 + \frac{1}{d_1} \int_t^{t+1} C ds \leq \frac{1}{2d_1} \left(1 + \frac{CC_1}{b_1} \right) + \frac{C}{d_1}, \text{ for } t > t_1.$$

Now we move to the L^2 estimate for the v component. This cannot be obtained directly. Thus we use the grouping method again by multiplying (6) by w_1 and (5) by w_0 , adding the two together, and setting $w = w_1 u + w_0 v$, we obtain:

$$(29) \quad w_t = d_2 \Delta w + (d_1 - d_2) w_1 \Delta u + w_1 a_1 u - w_1 b_1 u^2 - w_0 a_2 v - w_0 w_2 \left(\frac{vr}{v + D_2} \right).$$

We add a convenient zero, $-a_2 w_1 u + a_2 w_1 u$, to (29) to obtain

$$w_t = d_2 \Delta w + (d_1 - d_2) w_1 \Delta u + w_1 a_1 u - w_1 b_1 u^2 - a_2 w + a_2 w_1 u - w_0 w_2 \left(\frac{vr}{v + D_2} \right).$$

By multiplying (29) by w , integrating by parts over Ω , and keeping in mind the positivity of the solutions, we find that

$$\begin{aligned} & \frac{1}{2} \frac{d}{dt} \|w\|_2^2 + d_2 \|\nabla w\|_2^2 + a_2 \|w\|_2^2 \\ & \leq w_1(a_1 + a_2) \int_{\Omega} u w dx + \int_{\Omega} (d_2 - d_1) w_1 \nabla u \cdot \nabla w dx. \end{aligned}$$

This yields

$$\begin{aligned}
& \frac{d}{dt} \|w\|_2^2 + 2 \min(a_2, d_2) (\|\nabla w\|_2^2 + \|w\|_2^2) \\
& \leq 2w_1(a_1 + a_2) \int_{\Omega} u w dx + 2(d_2 - d_1)w_1 \int_{\Omega} \nabla u \cdot \nabla w dx \\
& \leq \min(a_2, d_2) \|w\|_2^2 + \frac{(2w_1(a_1 + a_2))^2}{2 \min(a_2, d_2)} \|u\|_2^2 + \min(a_2, d_2) \|\nabla w\|_2^2 \\
& \quad + \frac{(2(d_2 - d_1)w_1)^2}{2 \min(a_2, d_2)} \|\nabla u\|_2^2,
\end{aligned}$$

such that

$$\begin{aligned}
& \frac{d}{dt} \|w\|_2^2 + \min(a_2, d_2) (\|w\|_2^2 + \|\nabla w\|_2^2) \\
& \leq \frac{(2w_1(a_1 + a_2))^2}{2 \min(a_2, d_2)} \|u\|_2^2 + \frac{(2(d_2 - d_1)w_1)^2}{2 \min(a_2, d_2)} \|\nabla u\|_2^2.
\end{aligned}$$

Now via estimates in [42] we obtain

$$\|w\|_2^2 \leq C,$$

for $t > t_3$ where t_3 is explicitly derived in [42], $t_3 = \max \left\{ 0, \ln \left(\frac{w_1 \|u_0\|_2^2 + w_0 \|v_0\|_2^2}{C} \right) \right\}$ which implies that

$$\|v\|_2^2 \leq C, \text{ for } t > t_3.$$

Notice by multiplying (5) by v and integrating by parts one obtains,

$$\frac{1}{2} \frac{d}{dt} \|v\|_2^2 + d_2 \|\nabla v\|_2^2 + a_2 \|v\|_2^2 \leq w_1 \|v\|_2^2$$

Integrating the above on $[t_3, t_3 + 1]$ yields

$$\int_{t_3}^{t_3+1} \|\nabla v\|_2^2 ds \leq \int_{t_3}^{t_3+1} w_1 \|v\|_2^2 ds + \frac{1}{2} \|v(t_3)\|_2^2 \leq (w_1 + 1)C \leq C$$

Thus via the mean value theorem for integrals we obtain a time $t_3^* \in [t_3, t_3 + 1]$ s.t

$$\|\nabla v(t_3^*)\|_2^2 \leq C$$

In addition, we recap the uniform H^1 estimates found in [42],

$$(30) \quad \|\nabla u\|_2^2 \leq C,$$

for $t > T_1$, the H^1 compactification time of the solution. We next need to derive H^1 estimates for the v component. This is tricky, since when we multiply (5) by $-\Delta v$, integrate by parts, and then apply Young's inequality with epsilon we obtain

$$\frac{1}{2} \frac{d}{dt} \|\nabla v\|_2^2 + a_2 \|\nabla v\|_2^2 \leq w_1 \|v\|_2^2 + w_2 \|r\|_2^2$$

However, there is no global estimate on r , as it may possibly blow up, but we know that there is always a local solution on $[0, \frac{1}{2}T^*]$, where T^* is the blow up time of $r_t = d_3 \Delta r + cr^2$. Furthermore, on this time interval the solution is classical. Thus we make local in time estimates on this interval, using standard local in time

estimates on $\|r\|_\infty$ from [48]. Using Gronwall's inequality via integration on the time interval $[t_3^*, t]$ yields,

$$\begin{aligned} \|\nabla v\|_2^2 &\leq e^{-2a_2 t} \|\nabla v(t_3^*)\|_2^2 + \frac{1}{a_2} \left(w_1 C + w_2 C_1 \frac{c\|r_0\|_\infty}{d_3} \right) \\ &\leq 1 + \frac{1}{a_2} \left(w_1 C + w_2 C_1 \frac{c\|r_0\|_\infty}{d_3} \right) \end{aligned}$$

for $t > T_4 = \max \left\{ 0, \frac{\ln(\|\nabla v(t_3^*)\|_2^2)}{a_2}, t_3^* \right\}$.

Note, Lemma 4.3 requires us to manipulate a_2 , in order to prove large data global existence. From a practical point of view this is not always easy as manipulating the death rate directly may not be conducive to realistic control strategies. We next provide the following improved result that is valid even if $\|v_0\|_\infty \geq \frac{w_3}{c} - D_3$, without manipulating a_2 .

Theorem 4.4. *Consider the three-species food-chain model described by (4)-(6). For certain initial data $(u_0, v_0, r_0) \in L^2(\Omega)$, there exists a global classical solution (u, v, r) to the system, even if $\|v_0\|_\infty \geq \frac{w_3}{c} - D_3$, as long as the parameters are such that $\|v\|_\infty \leq \frac{w_3}{c} - D_3$, by the H^2 absorption time of v (denoted T_6). If T_6 satisfies $T_6 \leq T^*$, where T^* is the blow up time of the following PDE*

$$\partial_t r - d_3 \Delta r = cr^2.$$

with the same initial and boundary conditions as (4)

In order to show that blow up can be avoided as stated above, even in \mathbb{R}^2 our H^1 estimates via (30) must be improved. This is because the embedding of $H^1 \hookrightarrow L^\infty$ is lost in \mathbb{R}^2 . Thus, if we are to control the L^∞ norm in \mathbb{R}^2 we need H^2 control. This is achieved in the next subsection.

4.2.3. Uniform $H^2(\Omega)$ Estimates. We will estimate the H^2 norms via the following procedure, we rewrite (6) as

$$u_t - d_1 \Delta u = a_1 u - b_2 u^2 - w_0 \left(\frac{uv}{u + D_0} \right).$$

We square both sides of the equation and integrate by parts over Ω to obtain

$$\begin{aligned} &\|u_t\|_2^2 + d_1 \|\Delta u\|_2^2 + \frac{d}{dt} \|\nabla u\|_2^2 \\ &= \left\| \left(a_1 u - b_2 u^2 - w_0 \left(\frac{uv}{u + D_0} \right) \right) \right\|_2^2 \\ &\leq C \left((a_1)^2 \|u\|_2^2 + (w_0)^2 \|v\|_2^2 \right) + (b_2)^2 \|u\|_4^4 \leq C. \end{aligned}$$

This result follows by the embedding of $H^1 \hookrightarrow L^4 \hookrightarrow L^2$. Therefore, we obtain

$$\|u_t\|_2^2 + d_1 \|\Delta u\|_2^2 + \frac{d}{dt} \|\nabla u\|_2^2 \leq C.$$

Due to classical local in time regularity results, see 1, the solutions are $C^1(0, T; C^2(\Omega))$, thus $\frac{d}{dt} \|\nabla u\|_2^2$ cannot escape to $-\infty$, and is bounded below, upto the existence time. Thus we obtain

$$\|u_t\|_2^2 \leq C_1(t), \quad \|\Delta u\|_2^2 \leq C_2(t).$$

These constants may depend on t since even though $\frac{d}{dt} \|\nabla u\|_2^2$ cannot escape to $-\infty$ in finite time the case of it decaying like $-t$ is not precluded. We now make uniform

in time estimates of the higher order terms. Integrating the estimates of (32) in the time interval $[T, T+1]$, for $T > T_5 = \max(T_1, T_4)$, where T_5 is the maximum of the H^1 compactification times of u, v yields

$$\int_T^{T+1} \|u_t\|_2^2 dt \leq C_1, \quad \int_T^{T+1} \|\Delta u\|_2^2 dt \leq C_2.$$

Similarly we adopt the same procedure for v to obtain

$$\int_T^{T+1} \|v_t\|_2^2 dt \leq C_1, \quad \int_T^{T+1} \|\Delta v\|_2^2 dt \leq C_2.$$

However, the above estimates for v are made on the time interval $[0, \frac{T^*}{2}]$.

Next, consider the gradient of (6). Following the same technique as in deriving (32) we obtain for the left hand side

$$\begin{aligned} & \|\nabla u_t\|_2^2 + d_1 \|\nabla(\Delta u)\|_2^2 + \frac{d}{dt} \|\Delta u\|_2^2 + \int_{\partial\Omega} \Delta u \nabla u_t \cdot \mathbf{n} dS \\ &= \|\nabla u_t\|_2^2 + d_1 \|\nabla(\Delta u)\|_2^2 + \frac{d}{dt} \|\Delta u\|_2^2 + \int_{\partial\Omega} \Delta u \frac{\partial}{\partial t} (\nabla u \cdot \mathbf{n}) dS \\ (31) \quad &= \|\nabla u_t\|_2^2 + d_1 \|\nabla(\Delta u)\|_2^2 + \frac{d}{dt} \|\Delta u\|_2^2 \end{aligned}$$

This follows via the boundary condition. Thus we have

$$\begin{aligned} & \|\nabla u_t\|_2^2 + d_1 \|\nabla(\Delta u)\|_2^2 + \frac{d}{dt} \|\Delta u\|_2^2 \\ &= \left(\nabla(a_1 u - b_2 u^2 - w_0 \left(\frac{uv}{u + D_0} \right)) \right)^2 \\ (32) \quad & \leq C(\|u\|_4^4 + \|v\|_4^4 + \|\Delta u\|_2^2 + \|\Delta v\|_2^2) \end{aligned}$$

This follows via Young's inequality with epsilon, as well as the embedding of $H^2(\Omega) \hookrightarrow W^{1,4}(\Omega)$. This implies that

$$\frac{d}{dt} \|\Delta u\|_2^2 \leq C \|\Delta u\|_2^2 + C(\|u\|_4^4 + \|v\|_4^4 + \|\Delta v\|_2^2)$$

We now use the uniform Gronwall lemma with

$$\beta(t) = \|\Delta u\|_2^2, \quad \zeta(t) = C, \quad h(t) = C(\|u\|_4^4 + \|v\|_4^4 + \|\Delta v\|_2^2), \quad q = 1$$

to obtain

$$\|\Delta u\|_2 \leq C, \quad \|\Delta v\|_2 \leq C, \quad \text{for } t > T_6 = T_5 + 1$$

The estimate for v is derived similarly, but again we assume we are on $[0, \frac{T^*}{2}]$. Thus, via elliptic regularity,

$$(33) \quad \|u\|_{H^2} \leq C, \quad \|v\|_{H^2} \leq C, \quad \text{for } t > T_6$$

Since $H^2 \hookrightarrow L^\infty$ in \mathbb{R}^2 and \mathbb{R}^3 , the following estimate is valid in \mathbb{R}^2 and \mathbb{R}^3

$$(34) \quad \|u\|_\infty \leq C, \quad \|v\|_\infty \leq C, \quad \text{for } t > T_6$$

Thus even if the data is such that $\|v_0\|_\infty > \frac{w_3}{c} - D_3$, if the parameters and the data (r_0, v_0, u_0) are such that $\frac{w_3}{c} - D_3 < C_1 C$, (for the C in (34), where C_1 is the

embedding constant for $H^2(\Omega) \hookrightarrow L^\infty(\Omega)$) and

$$\begin{aligned} T_6(r_0, v_0, u_0) &< 1 + \max \left\{ 0, T_1, \frac{\ln(\|\nabla v(t_3^*)\|_2^2)}{a_2}, \ln \left(\frac{w_1 \|u_0\|_2^2 + w_0 \|v_0\|_2^2}{C} \right) + 1 \right\} \\ &< \frac{d_3}{c \|r_0\|_\infty} < T^*, \end{aligned}$$

then we obtain

$$\|v\|_\infty \leq \frac{w_3}{c} - D_3 < C, \text{ for } t > T_6.$$

Since $T_6 < T^*$ the solution to $\partial_t r - d_3 \Delta r = cr^2$, has not blown up yet, and since this is a supersolution to r solving (4), this r has definitely not blown up. However, from this point on the coefficient of r^2 in (4) is negative, as $\left(c - \frac{w_3}{v+D_3}\right) < \left(c - \frac{w_3}{\|v\|_\infty + D_3}\right) < 0$, hence r solving (4) can never blow up, from this point on. This proves Theorem 4.4.

4.3. Long Time Dynamics.

4.3.1. Gradient Estimates for the Time Derivatives. Now we assume there are globally existing solutions, and we aim to investigate the regularity of the omega limit set. Hence we assume we are working with initial data and parameters for which r is globally bounded. To begin, we obtain useful integral in time estimates. In particular, we integrate (32) in time from $[T, T+1]$ where $T > T_6$, the H^2 absorbing time, to obtain

$$\int_T^{T+1} \|\nabla u_t\|_2^2 dt \leq C(\|u\|_4^4 + \|v\|_4^4 + \|\Delta u\|_2^2 + \|\Delta v\|_2^2) + \|\Delta u(T)\|_2^2 \leq C.$$

Similarly, an estimate for ∇v_t can be established, namely

$$\int_T^{T+1} \|\nabla v_t\|_2^2 dt \leq C.$$

We now develop higher order estimates for the time derivatives. First, consider the partial derivative w.r.t t of equations (6), multiplying by $-\Delta u_t$, and integrate over Ω we obtain

$$\begin{aligned} \frac{d}{dt} \|\nabla u_t\|_2^2 + d_1 \|\Delta u_t\|_2^2 &= a_1 \|\nabla u_t\|_2^2 + b_2 \int_\Omega u(u_t) \Delta u_t dx + w_0 \int \frac{u}{u+D_0} v_t \Delta u_t dx \\ &\quad + w_0 \int_\Omega v(u_t) \Delta u_t \frac{D_0}{(u+D_0)^2} dx. \end{aligned}$$

Using Holder's inequality, Young's inequality with epsilon, and our earlier estimates yield

$$\begin{aligned} \frac{d}{dt} \|\nabla u_t\|_2^2 + d_1 \|\Delta u_t\|_2^2 &\leq a_1 \|\nabla u_t\|_2^2 + C \|u\|_\infty^2 \|u_t\|_2^2 + \frac{d_1}{4} \|\Delta u_t\|_2^2 + C_1 \|v_t\|_2^2 \\ &\quad + \frac{d_1}{4} \|\Delta u_t\|_2^2 + C_2 \|v\|_\infty \|u_t\|_2^2 + \frac{d_1}{4} \|\Delta u_t\|_2^2. \end{aligned}$$

Thus we obtain

$$\frac{d}{dt} \|\nabla u_t\|_2^2 \leq a_1 \|\nabla u_t\|_2^2 + C \|u\|_\infty^2 \|u_t\|_2^2 + C_1 \|v_t\|_2^2 + C_2 \|v\|_\infty \|u_t\|_2^2.$$

The application of the uniform Gronwall Lemma with

$$\begin{aligned}\beta(t) &= \|\nabla u_t\|_2^2, \quad \zeta(t) = a_1, \\ h(t) &= C\|u\|_\infty\|u_t\|_2^2 + C_1\|v_t\|_2^2 + C_2\|v\|_\infty\|u_t\|_2^2, \quad q = 1\end{aligned}$$

gives us the following uniform bound

$$(35) \quad \|\nabla u_t\|_2^2 \leq C, \quad t > T_7 = T_6 + 1$$

Similar methods applied to the equation for v and r yield

$$\|\nabla v_t\|_2^2 \leq C, \quad t > T_7, \quad \|\nabla r_t\|_2^2 \leq C, \quad t > T_7.$$

4.3.2. Regularity of the omega limit set. We now show that the asymptotic state $(0, v, u)$ under certain parameter restrictions is an attractor with more regularity than was derived previously. Essentially, we consider $(r_0, v_0, u_0) \in L^2(\Omega)$ for which we have globally existing solutions, that is the maximal existence time for the solutions $T = \infty$. Then we consider the omega limit set for such solutions.

$$(36) \quad \omega(r_0, v_0, u_0) = \overline{\bigcup_{t \geq 0} \{(r(s), v(s), u(s)) : s \geq t\}}$$

We state the following result.

Theorem 4.5. *Consider the three-species food-chain model described by (4)-(6). For initial conditions (r_0, v_0, u_0) , such that there is a globally existing solution, there exists a parameter a_2 , (depending on the initial condition), for which the omega limit set $\omega(r_0, v_0, u_0) = (0, v, u)$. Furthermore this is an attractor with $H^2(\Omega)$ regularity.*

Remark 5. Thus for suitably chosen a_2 , the attractor for such solutions is the extinction state of r .

Proof. We have shown that the system is well posed, under certain parameter, and data restrictions, via theorem 4.4. Thus, there exists a well-defined semigroup $\{S(t)\}_{t \geq 0} : H \rightarrow H$. Also, via Lemma 4.3 we can find an a_2 such that r decays to zero. The estimates via (33) establish the existence of bounded absorbing sets in H^2 . Now we rewrite the equation for a sequence u_n as follows

$$d_1 \Delta u_n = \partial_t u_n - a_1 u_n + b_2 u_n^2 + w_0 \left(\frac{u_n v_n}{u_n + D_0} \right),$$

We aim to show the convergence of both the right hand side strongly in L^2 . Due to the uniform bounds via (30), (35), (33) and the embedding of $H^1(\Omega) \hookrightarrow L^4(\Omega) \hookrightarrow L^2(\Omega)$ and $H^2(\Omega) \hookrightarrow L^\infty(\Omega)$ we obtain a subsequence u_{n_j} still labeled u_n s.t

$$\begin{aligned}\partial_t u_n &\xrightarrow{L^2} \partial_t u^*, \\ a_1 u_n &\xrightarrow{L^2} a_1 u^*, \\ b_2 u_n^2 &\xrightarrow{L^2} b_2 (u^*)^2\end{aligned}$$

as $\int_\Omega |(u_n - u^*)(u_n + u^*)|^2 dx \leq \|u_n + u^*\|_\infty \|u_n - u^*\|_2^2 \rightarrow 0$, as $u_n \xrightarrow{L^2} u^*$. Similarly,

$$w_0 \left(\frac{u_n v_n}{u_n + D_0} \right) \xrightarrow{L^2} w_0 \left(\frac{u^* v^*}{u^* + D_0} \right)$$

as $v_n \xrightarrow{L^2} v^*$. Thus, given a sequence $\{u_n(0)\}_{n=1}^\infty$ that is bounded in $L^2(\Omega)$, we know that, for $t > T_7$,

$$S(t_n)(\Delta u_n(0)) \rightarrow \Delta u^* \text{ in } L^2(\Omega).$$

This yields the precompactness in $H^2(\Omega)$, hence the closure in (36) is in $H^2(\Omega)$. A similar analysis can be done for the v and r components. Hence the theorem is established. \square

5. NUMERICAL APPROXIMATION

In this section a numerical approximation for the one and two dimensional models are developed in order to numerically demonstrate our earlier conjectures (1), (2), and (3) in addition to exploring the rich dynamics the mathematical models exhibit. A one-dimensional spectral-collocation method is developed to approximate the one dimensional equations (24)-(26) which include overcrowding, refuges, and role-reversal. We then offer a second order finite difference approximation of the two-dimensional equations (8), (9), and (6) that investigate the effect of a refuge. Overcrowding and role-reversal effects are not investigated in the latter numerical approximation. The two dimensional approximation employs a Peaceman-Rachford operator splitting and techniques developed by one of the authors in [5]. This approach takes advantage of the sparsity and structure of the underlying matrices and the known computational efficiency of operator splitting methods. Without loss of generality the domain is scaled and translated to $(-1, 1)$ and $(-1, 1) \times (-1, 1)$ in one and two-dimensions, respectively.

5.1. Approximation in One Dimension. We develop a spectral-collocation approximation of (24)-(26). These equations can be written compactly as

$$\mathbf{w}_t = \mathcal{L}\mathbf{w},$$

where $\mathbf{w} = (u, v, r)^\top$ and \mathcal{L} is the differential operator that includes the Laplacian operator and reactive terms.

The spatial approximation is constructed from a Chebychev collocation scheme [13, 25, 52]. The spatial approximation is constructed as a linear combination of the interpolating splines on the Gauss-Lobatto quadrature. The resulting system is then integrated in time using an implicit scheme, in particular a second order Adams-Moulton method. The Chebychev collocation approximation allows for a high order spatial approximation [25]. This offers the ability to capture fine resolution details with a relatively smaller number of degrees of freedom. However, there is a downside. The resulting matrices are full and ill conditioned [52]. This is problematic for the inversion in the resulting linear solve. Nevertheless, the spectrum associated with the second derivative operator is real, negative, and grows in magnitude like $O(N^4)$ [23, 25].

The collocation scheme is constructed on the Gauss-Lobatto abscissa with respect to the Chebychev weight,

$$(37) \quad x_j = \cos\left(\frac{j\pi}{N}\right),$$

where $j = 0, \dots, N$. An approximation is then constructed as a linear combination of the Lagrange interpolates on the abscissa,

$$(38) \quad \mathbf{w}_N(x, t) = \sum_{j=0}^N \mathbf{a}_j(t) \phi_j(x),$$

where $\mathbf{w}_N(x, t)$ is an approximation to the unknown populations and $\mathbf{a}_j(t)$ is a 3×1 vector of fourier coefficients. The basis functions are defined by

$$\begin{aligned} \phi_j(x) &= \frac{(-1)^{N+j+1}(1-x^2)T'_N(x)}{c_j N^2(x-x_j)}, \\ c_j &= \begin{cases} 2 & \text{if } j = 0, N, \\ 1 & \text{otherwise.} \end{cases}, \end{aligned}$$

and each $\phi_j(x)$ is a polynomial of degree N [25]. The basis functions also satisfy $\phi_j(x_i) = \delta_{ji}$. This is used to develop an approximation to our differential operator and a system of equations is constructed via a discrete inner product,

$$\langle \mathbf{w}_t, \phi_m \rangle_N = \langle P_N \mathcal{L} \mathbf{w}_N, \phi_m \rangle_N,$$

where P_N is the projection operator onto the space of polynomials of degree N . The discrete inner product is given below, and it is based on an inner product defined by

$$(39) \quad \langle u, v \rangle_w = \int_{-1}^1 \frac{u(x)v(x)}{\sqrt{1-x^2}} dx.$$

The integral can be approximated as a sum over the Gauss-Lobatto quadrature for the Chebychev weight and is exact for polynomials up to degree $2N-1$,

$$\int_{-1}^1 \frac{p_{2N-1}(x)}{\sqrt{1-x^2}} dx = \sum_{i=0}^N p_{2N-1}(x_i) w_i.$$

The resulting norm results in an equivalent norm for polynomials up to degree $2N$ [8]. The abscissa, x_i , are the same as those defined in equation (37), and the w_i are the quadrature weights. The resulting numerical approximation is then constructed using this finite inner product

$$\langle f, g \rangle_N = \sum_{i=0}^N f(x_i) g(x_i) w_i.$$

The resulting approximation is an extension of that given in (39) and is constructed using a Galerkin approach,

$$\begin{aligned} \langle \mathbf{w}_t, \phi_m \rangle_N &= \langle P_N \mathcal{L} \mathbf{w}_N, \phi_m \rangle_N, \\ \sum_{i=0}^N \frac{\partial}{\partial t} \mathbf{w}_N(x_i, t) \phi_m(x_i) w_i &= \sum_{i=0}^N P_N \mathcal{L} \mathbf{w}_N, \phi_m(x_i) w_i. \end{aligned}$$

The basis functions, $\phi_m(x)$, are Lagrange interpolants, and after substitution of the definition in equation (38) the result can be greatly simplified,

$$\mathbf{a}'_m(t) = P_N \mathcal{L} \mathbf{w}_N \Big|_{x=x_m},$$

where $m = 0, \dots, N$.

The Adams-Moulton method used to advance the initial value problem in time necessitates solving a nonlinear system of equations at each time step. This is achieved through a Newton-Raphson method. The ensuing linearized problem in the Newton-Raphson method is solved through a restarted GMRES [37].

5.2. Approximation in Two Dimensions. A second order approximation of (8), (9), and (6) is developed. While the spectral-Galerkin approximation of the previous section may be extended to two dimensions, the computational cost of the nonlinear solve is troublesome due to the sensitivity of the matrices and the lack of their sparsity. Here, the approximation is still of high order, while the underlying matrices are block tridiagonal or tridiagonal with diagonal blocks. This enables direct inversion techniques, in particular the Thomas algorithm.

The governing equations are written compactly as

$$\mathbf{w}_t = D\Delta\mathbf{w} + \mathbf{f},$$

where $\mathbf{w} = (u, v, r)^\top$, $\mathbf{f} = (f(\mathbf{w}, \mathbf{x}, t), g(\mathbf{w}, \mathbf{x}, t), h(\mathbf{w}, \mathbf{x}, t))^\top$ are the reactive terms that depend on space, time, and the species u, v , and r , $\mathbf{x} = (x, y)$, $\Delta\mathbf{w}$ is taken component-wise, and D is a diagonal matrix with nonnegative entries d_1 , d_2 , and d_3 . From semigroup theory the formal solution is

$$\mathbf{w}(\mathbf{x}, t) = \exp(tD\Delta)\mathbf{w}(\mathbf{x}, 0) + \int_0^t \exp\{(t-\tau)\Delta\}\mathbf{f}(\mathbf{x}, \tau)d\tau,$$

where $\exp\{\}$ is the evolution operator associated with D . A suitable quadrature is used to approximate the integral. Here, a second order trapezoidal rule is used, that is,

$$\mathbf{w}(\mathbf{x}, t) = \exp(tD\Delta)\left(\mathbf{w}(\mathbf{x}, 0) + \frac{t}{2}\mathbf{f}(\mathbf{x}, 0)\right) + \frac{t}{2}\mathbf{f}(\mathbf{x}, t) + O(\delta t^2).$$

This motivates the implicit method,

$$\begin{aligned} \mathbf{w}(\mathbf{x}, t_{k+1}) &= \exp(tD\Delta)\left(\mathbf{w}(\mathbf{x}, t_k) + \frac{\delta t}{2}\mathbf{f}(\mathbf{x}, t_k)\right) \\ &\quad + \frac{\delta t}{2}\mathbf{f}(\mathbf{x}, t_{k+1}) + O(\delta t^2), \end{aligned}$$

where $t_{k+1} = t_k + \delta t$. The exponential is approximated through a Peaceman-Rachford operator. This creates the second order implicit method,

$$\begin{aligned} \mathbf{w}(\mathbf{x}, t_{k+1}) &= \left(I - \frac{\delta t_k}{2}B\right)^{-1}\left(I - \frac{\delta t_k}{2}A\right)^{-1}\left(I + \frac{\delta t_k}{2}A\right)\left(I + \frac{\delta t_k}{2}B\right)\left(\mathbf{w}(\mathbf{x}, t_k) \right. \\ &\quad \left. + \frac{\delta t_k}{2}\mathbf{f}(\mathbf{x}, t_k)\right) + \frac{\delta t_k}{2}\mathbf{f}(\mathbf{x}, t_{k+1}) + O(\delta t_k^2), \end{aligned}$$

where δt_k is the variable time step, $A = \frac{\partial^2}{\partial x^2}$, and $B = \frac{\partial^2}{\partial y^2}$. The last reactive term does require the solution at the next time step. To avoid a required nonlinear solve, we use a first order approximation to avoid this. This simplification maintains the second order accuracy of the approximation. We write the solution in an alternative form,

$$\begin{aligned} \left(I - \frac{\delta t_k}{2}A\right)\left(I - \frac{\delta t_k}{2}B\right)\mathbf{w}(\mathbf{x}, t_{k+1}) &= \left(I + \frac{\delta t_k}{2}A\right)\left(I + \frac{\delta t_k}{2}B\right)\left(\mathbf{w}(\mathbf{x}, t_k) + \frac{\delta t_k}{2}\mathbf{f}(\mathbf{x}, t_k)\right) \\ &\quad + \frac{\delta t_k}{2}\left(I - \frac{\delta t_k}{2}A\right)\left(I - \frac{\delta t_k}{2}B\right)\mathbf{f}(\mathbf{x}, t_{k+1}) + O(\delta t_k^2), \end{aligned}$$

This can be conveniently solved through ADI procedures [59], that is, by splitting the problem into,

$$\begin{aligned} \left(I - \frac{\delta t_k}{2} A\right) \tilde{\mathbf{w}}(\mathbf{x}, t_{k+1}) &= \left(I + \frac{\delta t_k}{2} B\right) \mathbf{w}(\mathbf{x}, t_k) + \frac{\delta t_k}{2} \mathbf{f}(\mathbf{x}, t_k) \\ \left(I - \frac{\delta t_k}{2} B\right) \tilde{\mathbf{w}}(\mathbf{x}, t_{k+1}) &= \left(I + \frac{\delta t_k}{2} A\right) \tilde{\mathbf{w}}(\mathbf{x}, t_k) + \frac{\delta t_k}{2} \mathbf{f}(\mathbf{x}, t_{k+1}). \end{aligned}$$

We see that the first equation keeps A implicit while B is explicit. We then take our intermediate solution, $\tilde{\mathbf{w}}$, and solve the second equation keeping B implicit and A explicit. Now, the spatial operators may be approximated through the two-dimensional Chebyshev approximation similar to that of the previous section, however we choose second order central differences. Let $x_i = -1 + ih_x$ and $y_j = -1 + jh_y$, where $h_x = 2/(N-1)$, $h_y = 2/(M-1)$, for $i = 0, \dots, N-1$, and $j = 0, \dots, M-1$. Let A_h and B_h be the second order approximations to the operators A and B . The approximation is utilized throughout the entire two-dimensional domain. At the boundary, we require an equation for \mathbf{w} at *ghost* points, that is locations of x_{-1} , y_{-1} , x_{M+1} and y_{M+1} . These are established using central difference approximations to the Neumann boundary conditions. We then substitute these back into the system of equations. This maintains the second order accuracy and the tridiagonal structure of the equations. At each step, the tridiagonal equations in the ADI method are directly solved using the Thomas algorithm which comes at a expense of $O(NM)$.

5.3. Numerical Results. We numerically demonstrate that there is good evidence for conjectures (1), (2), and (3). In the one dimensional setting, we translate and scale the domain to $(0, \pi)$ and use a refuge function of

$$b_1(x) = \frac{1 - \tanh\left(\frac{x-a}{.04}\right)}{2}$$

The refuge size is delineated by the value a since that is the location where the gradient is steepest. As expected the blow up time is affected by the presence of a refuge. For instance, for a fixed parameter set we look at the effect on the blow up time with a refuge, refuge with role reversal, and role reversal and overcrowding as compared to the classical model. The results are shown in Figure 3.

Interestingly, in the modified model with role reversal, it is found that blow up does not occur when $b_1(x) = 0$ or $b_1(x) = 1, \forall x$ in the spatial domain.

We also see that the blow up times are influenced by the size of the refuge. In fact, there is critical refuge size for which given any refuge size greater then the solutions will not blow up. This is evidenced in Figure 3 by the steep gradient of the curves around 2.8. Therefore, the population of the invasive species can be controlled. In situations where there is only a spatial refuge the blow up time curve is always increasing. This is consistent with our two dimensional results.

It is clear that there exists a critical refuge size for which refuges larger than this will prevent blow up. In the one-dimensional model, without role reversal or overcrowding effects, we investigate the effect of the critical refuge size versus the size of the initial condition of v while maintaining the other initial conditions and parameters values. We use the same parameters as given in Figure 3 and vary the uniform initial condition on v . Interestingly, Figure 4 shows a logarithmic dependency of the critical refuge size to prevent blow-up of r , on the initial condition size of v .

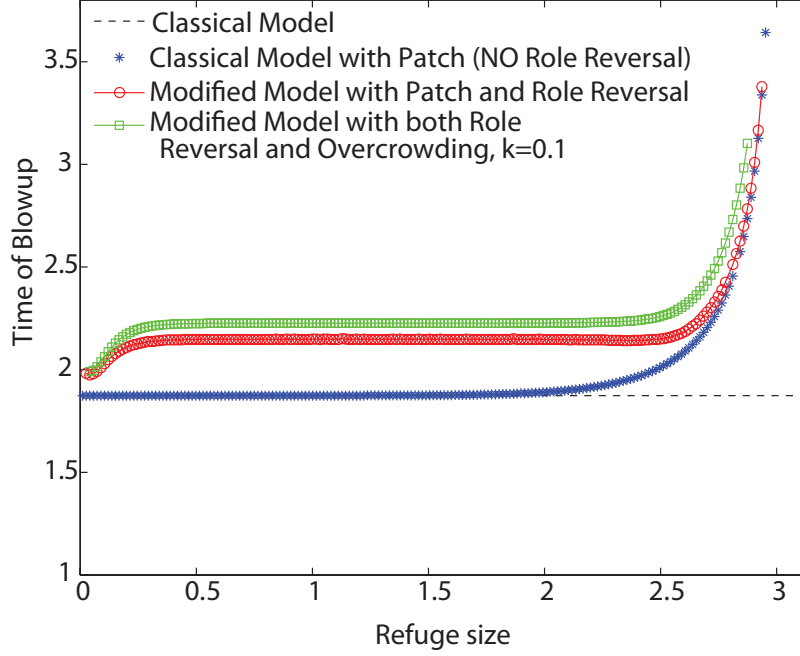


FIGURE 3. This shows blow up times for the classical model ($b_1(x) = 0$ and $d_4 = 0$) versus the modified model with the various biological controls. One sees that there is a critical patch size, such that for patches of length greater than this, there is no blow up. Inclusion of the overcrowding term, greatly decreases this critical size. The parameters used are $a_1 = 1$, $a_2 = 1$, $b_2 = 0.5$; $D_0 = 10$, $D_1 = 13$, $D_2 = 10$, $D_3 = 20$, $D_4 = D_2$, $c = 0.055$, $w_0 = 0.55$, $w_1 = 0.1$, $w_2 = 0.25$, $w_3 = 1.2$, $w_4 = 100$, $w_5 = 0.55$, $d_3 = d_2 = d_1 = .1$, $d_4 = k|c - \frac{w_3}{D_3}|$, where k is given in the plot. The initial conditions used are $u(x, 0) = r(x, 0) = 10$ and $v(x, 0) = 2000$. 128 grid points were used with a temporal step size of 10^{-3} . In the case of overcrowding and role reversal, as we increase the value of k similar results were observed.

The size of the spatial refuge has an influence on the blow up time. However, the location and number of spatial refuges also influences the blow up time. In fact, blow up is sometimes eliminated depending on the initial condition, refuges, and their subsequent locations. For instance, if we consider a uniform initial condition in r and compare the blow up time in a situation of a single refuge of width located near the boundary versus the case of evenly splitting this refuge then we find the blow up time is increased. This delay is exasperated if the two refuges are farther apart. Of course, if we consider a different initial condition then blow may not just be delayed, rather removed! For instance if we consider a concentrated initial population of r for which the highest concentration of r contains the spatial refuge then blow up can be eliminated! Hence, the concentration of r inside the refuge may protect the species enough so that the population of r decays sufficiently to avoid blow up in its population.

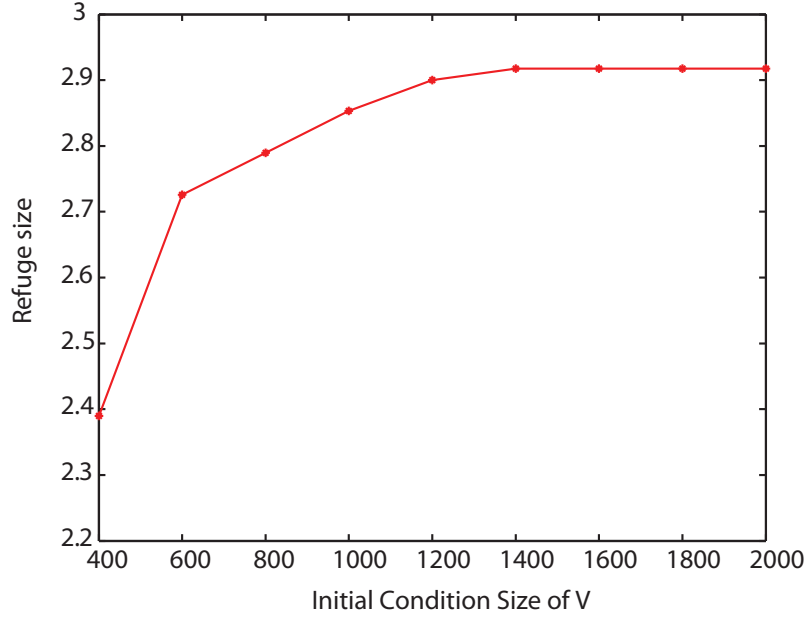


FIGURE 4. This shows a plot of the critical patch size for a given initial uniform condition size of v for which blow up in the invasive specie population r will occur. Identical parameters and resolution are used as in Figure 3. The domain was translated and scaled to $(0, \pi)$.

To illustrate this consider the two-dimensional model (8), (9), and (6) with an initial condition of

$$\begin{aligned} u(x, y, 0) &= \cos(2\pi x) \cos(2\pi y) + 30, \\ v(x, y, 0) &= u(x, y, 0) + 200, \\ r(x, y, 0) &= 100 \exp(-10(x^2 + y^2)), \end{aligned}$$

with parameters $d_1 = d_2 = d_3 = .1$, $a_1 = 5$, $a_2 = .75$, $b_2 = .5$, $w_0 = .55$, $w_1 = 1$, $w_2 = .25$, $w_3 = 1.2$, $c = .055$, $D_0 = 20$, $D_1 = 13$, $D_2 = 10$, $D_3 = 20$. Clearly, the coefficient $c - \frac{w_3}{D_3} < 0$. If $b_1(x, y)$ is zero throughout the entire spatial domain there exists blow up in the r population. However, if we have a circular refuge such that,

$$b_1(x, y) = \begin{cases} 1 & x^2 + y^2 < R \\ 0 & \text{else} \end{cases},$$

for $R = .5$ then blow up is avoided. Figure 5 shows the total population versus time. We can see the population starts to increase rapidly, but the increase is attenuated as a result of the spatial refuge. Hence, the population growth is not sustained and begins to decrease. Hence, the size **and** location of the refuge and the initial condition play a delicate balance in preventing blow up.

In two dimensions if we choose a particular shape of the spatial refuge it was conjectured that there exists a critical size for which blow up is avoided. Here, we look at two situations: a square and circular refuges with increasing size centered in the middle of the spatial domain. We let $b_1(\mathbf{x}) = 1$ inside the refuge while 0 outside. This clearly delineates the protection zones. For a fixed parameter regime

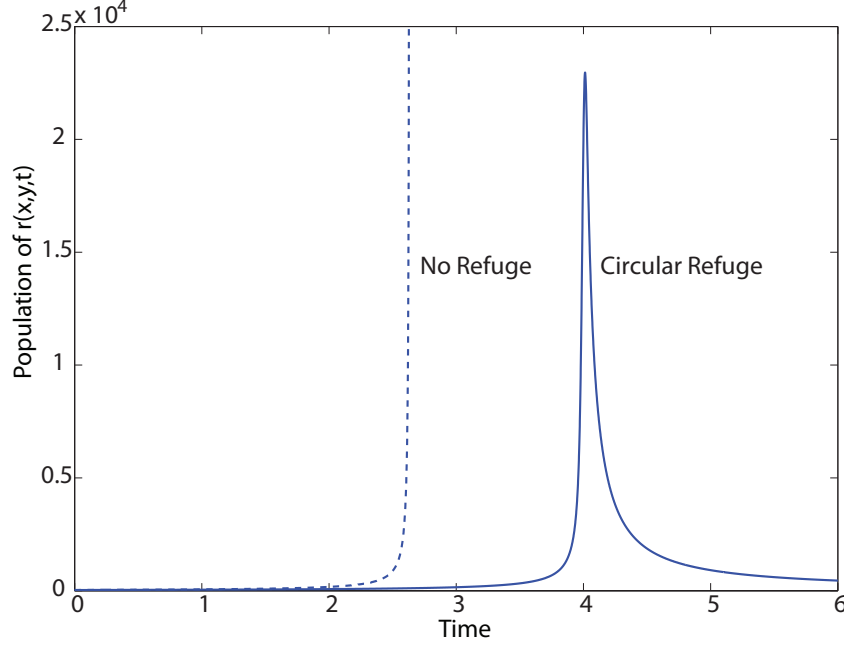


FIGURE 5. The population of $r(x, y, t)$, that is, $\int_{\Omega} r(x, y, t) d\Omega$, is shown versus time. With a circular refuge, we see that blow up is avoided. This provides experimental evidence that the location and size of the refuge is important to avoid blow up in the invasive population. The dashed line represents the population in the case where there is no spatial refuge. The simulations were done on a 50×50 uniform grid with a temporal step of .0001.

and initial conditions of

$$\begin{aligned} u(x, y, 0) &= r(x, y, 0) = \cos(2\pi x) \cos(2\pi y) + 30, \\ v(x, y, 0) &= \cos(2\pi x) \cos(2\pi y) + 230, \end{aligned}$$

we determine the critical refuge size. Each calculation is carried out with a 50×50 grid. The temporal step was fixed at .001. The parameters used: $d_1 = d_2 = d_3 = .1$, $a_1 = 1$, $b_1 = .5$, $w_0 = .55$, $w_1 = 2$, $w_2 = .25$, $w_3 = 1.2$, $c = .055$, $D_0 = 20$, $D_1 = 13$, $D_2 = 10$, $D_3 = 20$. It is found that for a square the critical refuge area is 2.5004, roughly 62.5% of the spatial domain. The critical refuge area for the circular refuge is approximately 2.6661, roughly 66.7% of the spatial domain.

6. SPATIO-TEMPORAL DYNAMICS

6.1. Turing Instability: Effect of Overcrowding on Turing Patterns. In this section we shall investigate the effects of overcrowding in the absence of refuges and role reversal, in the classical model. Therefore, we focus on whether an appropriate choice of d_4 can induce Turing Instabilities. It is shown in [43] that diffusion processes can destabilize the homogenous steady state solution when $d_4 = 0$. For convenience, we restate the one-dimensional model given in equations (6), (21), and

(22),

$$(40) \quad \frac{\partial u}{\partial t} = d_1 u_{xx} + a_1 u - b_2 u^2 - w_0 \left(\frac{uv}{u + D_0} \right),$$

$$(41) \quad \frac{\partial v}{\partial t} = d_2 v_{xx} - a_2 v + w_1 \left(\frac{uv}{u + D_1} \right) - w_2 \left(\frac{vr}{v + D_2} \right),$$

$$(42) \quad \frac{\partial r}{\partial t} = d_3 r_{xx} + cr^2 - w_3 \frac{r^2}{v + D_3} + d_4 (r^2)_{xx}.$$

Consider the linearization of (40)-(42) about the positive interior equilibrium point

$$E_6 = (u^*, v^*, r^*),$$

where $u^* = \frac{a_1 - b_2 D_0}{2b_2} + \sqrt{\left(\frac{a_1 - b_2 D_0}{2b_2}\right)^2 - \left(\frac{w_0 v^* - a_1 D_0}{b_2}\right)}$, v^* is the the spatially homogeneous steady state solution, and $r^* = \frac{v^* + D_2}{w_2} \left(\frac{w_1 u^*}{u^* + D_1} - a_2 \right)$ (see [43]). For instance, for the parameters given at the beginning of this section $u^* = 10.110031$, $v^* = 10$, and $r^* = 2.997897$. Consider a small space time perturbation, that is,

$$\mathbf{W} = U - U^* = O(\epsilon), \text{ where } \epsilon \rightarrow 0,$$

with U^* as the positive interior equilibrium point given as E_6 and $U = (u, v, r)$. Substituting and collecting linear terms of order $O(\mathbf{W})$, we obtain

$$\begin{aligned} \frac{\partial \mathbf{W}}{\partial t} &= \mathbf{D} \Delta \mathbf{W} + \mathbf{J} \mathbf{W}, \\ \Delta \mathbf{W}_i \cdot \mathbf{n} &= 0 \quad \text{for } x \in \partial \Omega, i = 1, 2, 3. \end{aligned}$$

where

$$\mathbf{D}_{u^*, v^*, r^*} = \begin{bmatrix} d_1 & 0 & 0 \\ 0 & d_2 & 0 \\ 0 & 0 & d_3 + 2d_4 r^* \end{bmatrix},$$

is the diffusion matrix and

$$\mathbf{J}_{u^*, v^*, r^*} = \begin{bmatrix} u^* \left(-b_2 + \frac{w_0 v^*}{(u^* + D_0)^2} \right) & -\frac{u^* w_0}{u^* + D_0} & 0 \\ \frac{v^* D_1 w_1}{(u^* + D_1)^2} & \frac{v^* w_2 r^*}{(v^* + D_2)^2} & -\frac{v^* w_2}{v^* + D_2} \\ 0 & \frac{r^{*2} w_3}{(v^* + D_3)^2} & 0 \end{bmatrix} = \begin{bmatrix} A_{11} & A_{12} & A_{13} \\ A_{21} & A_{22} & A_{23} \\ A_{31} & A_{32} & A_{33} \end{bmatrix},$$

is the Jacobian matrix associated with the ordinary differential equation part of model (40)-(42).

Let

$$\mathbf{W}(\varepsilon, t) = \begin{bmatrix} \bar{u}_0 \\ \bar{u}_1 \\ \bar{u}_2 \end{bmatrix} e^{\lambda t + ik\varepsilon},$$

where ε is the spatial coordinate in Ω , $\bar{u}_i (i = 0, 1, 2)$ is the amplitude, λ is the eigenvalues associated with the interior equilibrium point, E_6 and k is the wave number of the solution. Upon substituting, we obtain the characteristic equation

$$(43) \quad |\mathbf{J} - \lambda \mathbf{I} - k^2 \mathbf{D}| = 0,$$

where \mathbf{I} is a 3×3 identity matrix. The sign of $Re(\lambda)$ indicates the stability, or lack thereof, of the equilibrium point E_6 . The dispersion relation is

$$P(\lambda) = A_3(k^2)\lambda^3 + A_2(k^2)\lambda^2 + A_1(k^2)\lambda + A_0(k^2).$$

The coefficients of $P(\lambda)$ are determined by expanding (43), namely,

$$\begin{aligned}
A_3(k^2) &= 1, \\
A_2(k^2) &= (d_1 + d_2 + (d_3 + 2d_4r^*))k^2 - A_{11} - A_{22} - A_{33}, \\
A_1(k^2) &= A_{22}A_{33} - A_{22}(d_3 + 2d_4r^*)k^2 - A_{23}A_{32} - A_{12}A_{21} - d_2A_{33}k^2 \\
&\quad + d_2(d_3 + 2d_4r^*)k^4 + \left((d_1k^2 - A_{11})(d_2k^2 + (d_3 + 2d_4r^*)k^2 \right. \\
&\quad \left. - A_{22} - A_{33}) \right), \\
A_0(k^2) &= \left((d_1k^2 - A_{11})(A_{22}A_{33} - A_{22}(d_3 + 2d_4r^*)k^2 - A_{23}A_{32} - A_{33}d_2k^2 \right. \\
&\quad \left. + d_2(d_3 + 2d_4r^*)k^4) \right) - A_{12}A_{21}(d_3 + 2d_4r^*)k^2 + A_{12}A_{21}A_{33}.
\end{aligned}$$

To check for stability of the equilibrium solution E_6 , we use the Routh Hurwitz criterion. This state that for E_6 to be stable we need

$$(44) \quad A_n(k^2) > 0, \forall n \quad \text{and} \quad A_1(k^2)A_2(k^2) > A_0(k^2).$$

Contradicting either of these statements ensures instability for E_6 . Finally, for diffusion to cause a Turing instability it is sufficient to require that around the equilibrium point we have

$$\begin{aligned}
\operatorname{Re}(\lambda(k=0)) &< 0, \quad \text{and} \\
\operatorname{Re}(\lambda(k>0)) &> 0.
\end{aligned}$$

We refer the reader to a well detailed analysis of this in [22]. Hence, for a Turing instability to occur, we require that (44) is satisfied when $k=0$ (without diffusion) and at least one of the equations in (44) changes sign when $k>0$ (with diffusion). By this we consider letting $A_0(k^2)$ become negative when $k>0$ and satisfy (44) when $k=0$. This suggests that spatial patterns should be observed. Our parameter search has not yielded a parameter set for which (44) holds while $d_4=0$. When $d_4>0$, at least one of these inequalities changes sign. Thus we cannot conclusively say that d_4 will induce or inhibit Turing pattern. However, it is conclusive that d_4 certainly has an effect on the type of patterns that do form. In particular, the patterns fall into two types: spatial patterns and spatio-temporal patterns. The conditions for which type forms is succinctly described via Table 1.

Case	A_0	$A_2A_1 - A_0$	A_1	Pattern Type
1	+	-	-	spatio-temporal
2	-	+	+	fixed spatial

TABLE 1. Conditions on the signs of coefficients for different types of patterns.

Now when $d_4>0$ this clearly changes the spatio-temporal pattern, as evidenced by the sign changes from Case 1 to 2 in Table 1. In this situation the dispersion relation is shown in Figure 6. The resulting patterns are shown Figure 7(a)-(f).

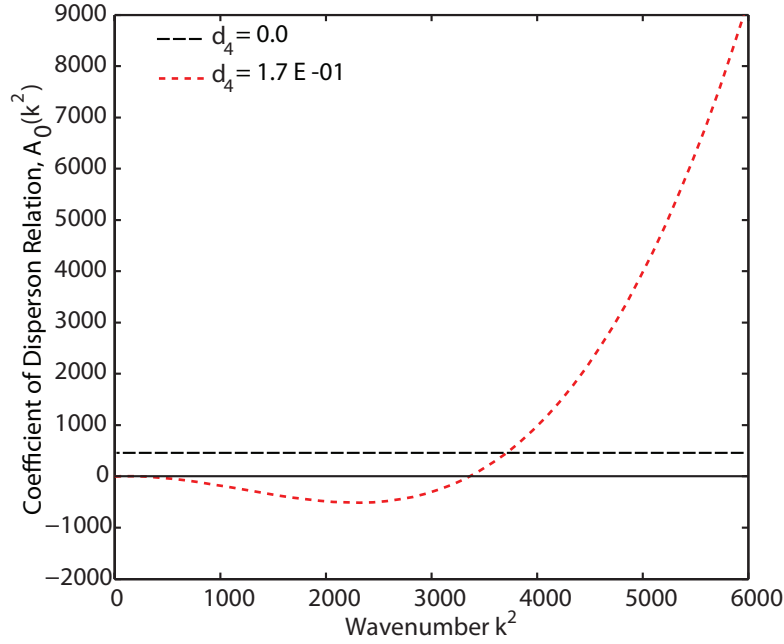


FIGURE 6. Dispersion Plot for two choices of d_4 resembling the two cases in Table 1. Notice that when $d_4 > 0$ a band of wavenumbers are unstable.

Remark 6. If $r = 0$ then (40)-(41) reduces to a model similar to the classical predator-prey model with a Holling type II functional response, for which we know there cannot occur Turing instability. There is one caveat, the death rate in v now becomes nonlinear. So essentially the equations are

$$(45) \quad \partial_t v = d_2 v_{xx} - \left(a_2 + w_2 \frac{r^*}{v + D_2} \right) v + w_1 \frac{uv}{u + D_1},$$

$$(46) \quad \partial_t u = d_1 u_{xx} + a_1 u - b_2 u^2 - w_0 \frac{uv}{u + D_0}.$$

Such systems have been investigated with and without cross and self diffusion [67]. In the regular diffusion case, it is known that a Turing instability can exist [56], where the nonlinearity in death rate is due to cannibalism. However, to our knowledge, for the specific form of the death rate as above this is not yet known.

Thus we see that the classical model (4)-(6) can exhibit spatio-temporal patterns, apart from just the spatial patterns that were uncovered in [43]. Furthermore addition of the overcrowding term in (4)-(6), can cause the spatio-temporal patterns to change into a purely spatial patterns. It is noted that the inclusion of overcrowding with a nonlinear death rate, such as in (45), can lead to Turing instability in the classical predator-prey model with Holling type II response.

6.2. Spatio-temporal chaos. The goal of this section is to investigate spatio-temporal chaos in the classical model (4)-(6). Spatio-temporal chaos is usually defined as deterministic dynamics in spatially extended systems that are characterized by an apparent randomness in space and time [11]. There is a large literature

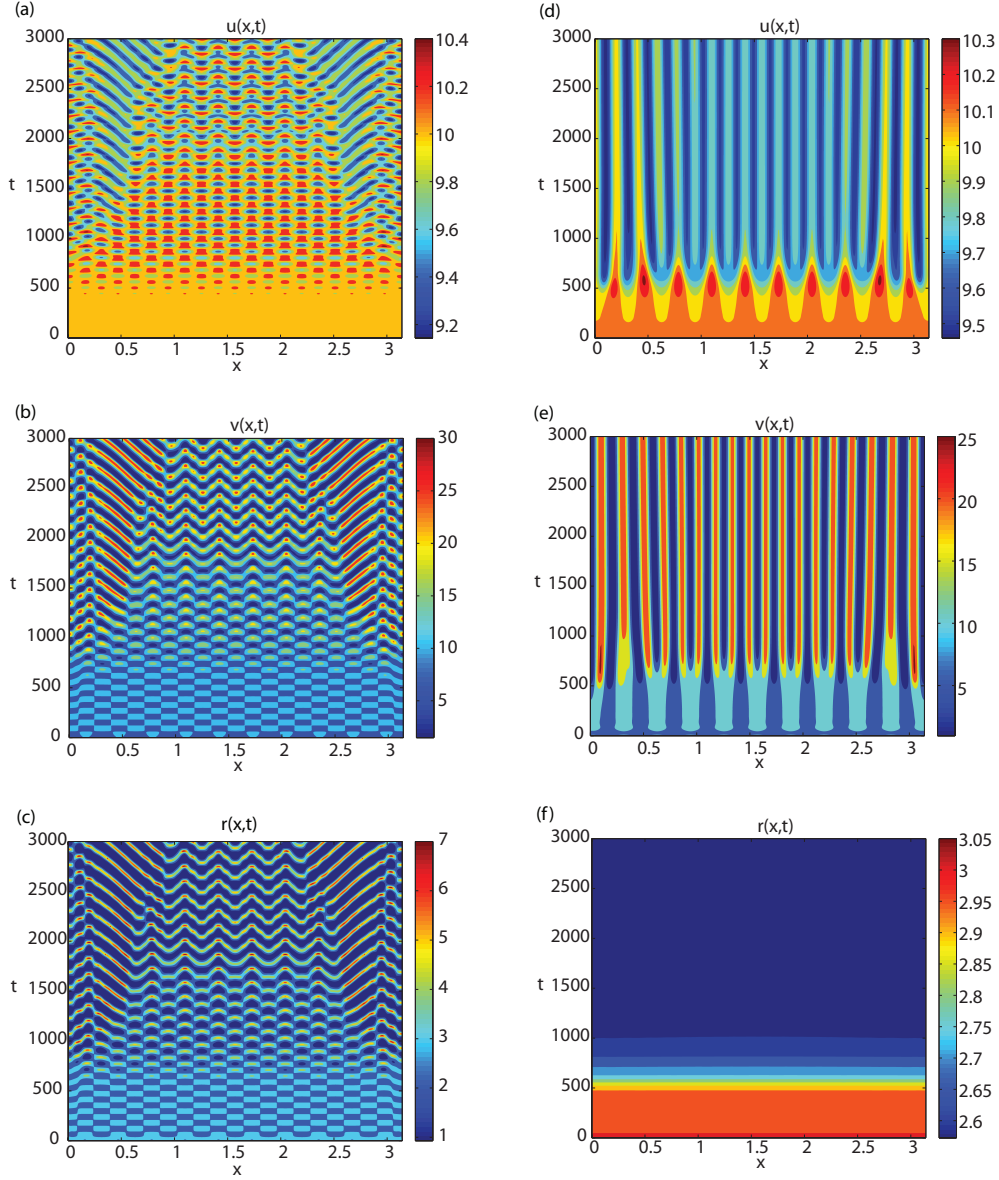


FIGURE 7. The densities of the three species are shown as contour plots in the xt -plane. The long-time simulation yields (a)-(c) Turing patterns ($d_4 = 0$), that are spatio-temporal, and (d)-(f) stripe Turing patterns ($d_4 = 1.6 \times 10^{-1}$), which are purely spatial. The other parameters are: $d_1 = 10^{-2}$, $d_2 = 10^{-5}$, $d_3 = 10^{-7}$, $a_1 = 1.79$, $a_2 = 0.8$, $b_2 = 0.15$, $c = 0.04$, $w_0 = 0.55$, $w_1 = 2$, $w_2 = 0.5$, $w_3 = 1.2$, $D_0 = 10$, $D_1 = 13$, $D_2 = 10$, $D_3 = 20$. 128 grid points are used with a temporal step size of .01.

on spatio-temporal chaos in PDE, in particular there has been a recent interest on spatially extended systems in ecology exhibiting spatio-temporal chaos [31]. However, most of these works are on two species models, and there is not much literature in the three-species case. In [43] we showed diffusion induced temporal chaos in (4)-(6), as well as spatial chaos when the domain is enlarged. In [32], various patterns non-Turing were uncovered in (4)-(6), in the case of equal diffusion, but spatio-temporal chaos was not confirmed. Note, that the appearance of a jagged structure in the species density, as seen in [32], which seems to change in time in an irregular way, does not necessarily mean that the dynamics is chaotic. One rigorous definition of chaos means sensitivity to initial conditions. Thus two initial distribution, close together, should yield an exponentially growing difference in the species distribution at later time. In order to confirm this in (4)-(6), we perform a number of tests as in [31]. We run (4)-(6) from a number of different initial conditions, that are the same modulo a small perturbation. The parameter set is chosen as in [32]. We then look at the difference of the two densities, at each time step in both the L^∞ and L^1 norms.

Thus we solve (4)-(6) with the following parameter set: $d_1 = 10^{-5}$, $d_2 = 10^{-5}$, $d_3 = 10^{-5}$, $a_1 = 1.93$, $a_2 = 1.89$, $b_2 = 0.06$, $c = 0.03$, $w_0 = 1$, $w_1 = 0.5$, $w_2 = 0.405$, $w_3 = 1$, $D_0 = 10$, $D_1 = 10$, $D_2 = 10$, $D_3 = 20$. Thus the steady state solution for the ODE system is $u^* = 25$, $v^* = 13$, $r^* = 9$.

The simulations use two different (but close together in $L^1(\Omega)$, $L^2(\Omega)$, $L^\infty(\Omega)$ norms) initial conditions. The first simulation (which we call r_{unpert}) is a perturbation of (r^*, v^*, u^*) by $0.1 \cos^2(x)$. The second simulation (which we call r_{pert}) is a perturbation of (r^*, v^*, u^*) by $0.11 \cos^2(x)$. The densities of the species are calculated up to the time $t = 5000$. At each time step in the simulation we compute

$$d(t) = \|r_{unpert}(x, t) - r_{pert}(x, t)\|_X,$$

where $X = L^1(\Omega)$, $L^2(\Omega)$ and $L^\infty(\Omega)$ are used. Then, $d(t)$ is plotted on a log scale. In doing so, we observe the exponential growth of the error. This grows at an approximate rate of $0.018 > 0$. Since this is positive then this is an indicator of spatio-temporal chaos. These numerical tests provide experimental evidence to the presence of spatio-temporal chaos in the classical model (4)-(6). Figure 8 shows the densities of the populations in the xt -plane while Figure 9 gives the error and its logarithm till $t = 1000$.

7. CONCLUSION

In this work we have proposed and investigated a new model for the control of an invasive population. An invasive species population is said to reach catastrophic population levels when its population reaches a particular threshold. The mathematical model uses the mathematical construct of finite time blow up which enables the model to examine the effect of controls for any particular threshold, especially since this level depends on the application. In effect, this construct demonstrates that if the invasive population has large enough numbers initially, it can grow to explosive levels in finite time: thus wreaking havoc on the ecosystem. Hence, we are interested in the influence certain controls will have on the invasive population and if its population may be reduced below disastrous levels. This formulation yields a clear mathematical problem: Assume that (4)-(6) blows-up in finite time for $c < \frac{w_3}{D_3}$ for a given initial condition. Are there controls and features of the

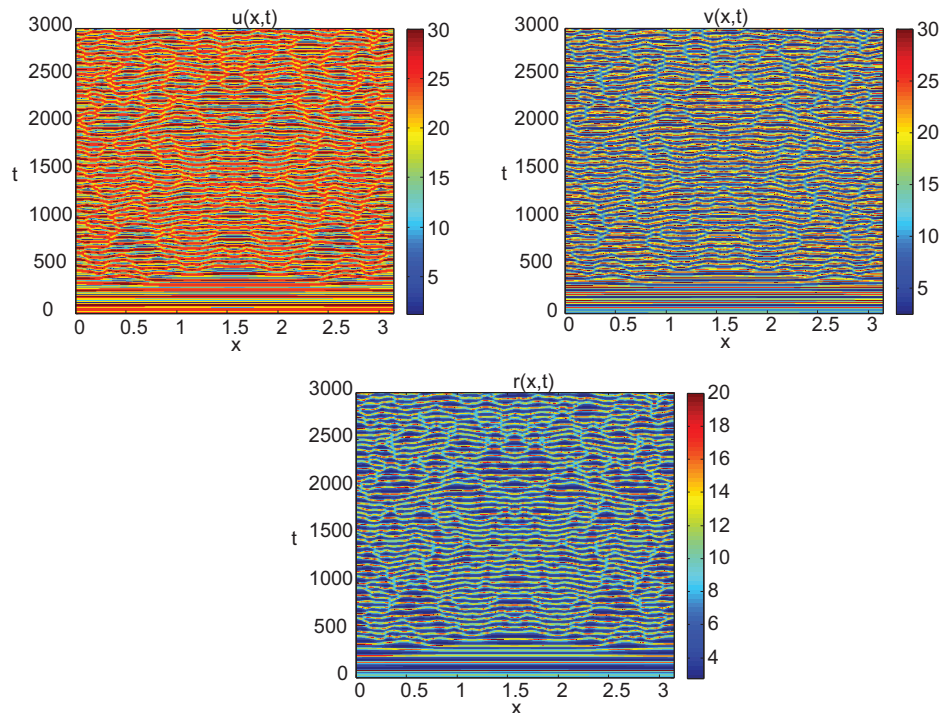


FIGURE 8. The densities of the three species are shown as contour plots in the xt -plane for u , v , and r from left to right. The long-time simulation yields spatio-temporal chaotic patterns. 128 grid points are used with a temporal step size of .01.

model that we can include to modify (4)-(6) so that now *there is no blow up* in the invasive population given the same initial condition? This paper addresses this question, suggesting clear controls and improvements to the mathematical model. We then investigate these improvements numerically and theoretically.

In traditional practice, biological control works on the enemy release hypothesis. That is releasing an enemy of the invasive species into the ecosystem will lead to a decrease in the invasive population. However, non-target effects are prevalent, hence this approach is problematic and may create even more devastating impacts on the ecosystem [16]. Here, we propose controls that do not use the release of biological agents. In particular, we introduce spatial refuges or safe zones for the primary food source of the invasive species. Mathematically, this transforms (4)-(6) into an indefinite problem [21], that is, where the sign of the coefficient of r^2 switches between inside and outside of the refuge. We demonstrated numerically and in analytically, with some assumptions, that this control can prevent blow up and drive the invasive population down. Our numerical experiments suggests that there is a delicate balance between the size and location of the refuge and the initial condition. In particular, we revealed a logarithmic dependence on the size of the initial condition for v versus the critical refuge size to prevent blow-up of r , see

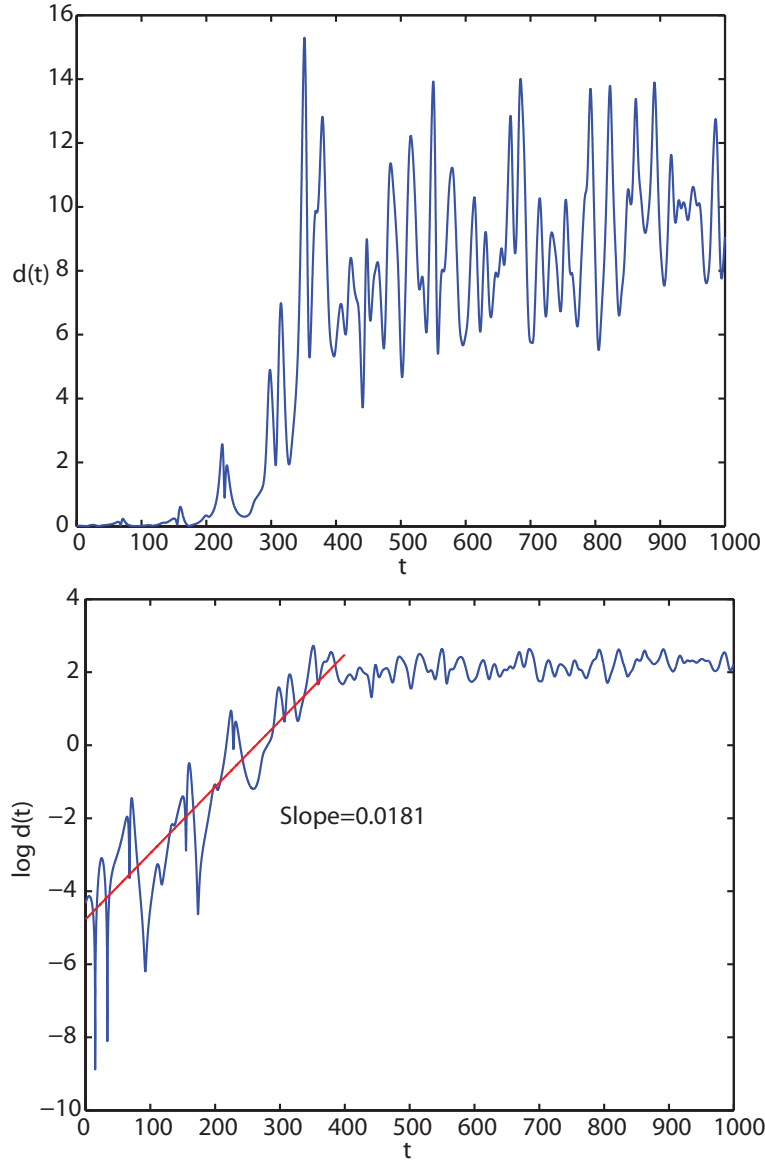


FIGURE 9. The difference $d(t)$ and its logarithm in the L^2 norm for the r species, under slightly different initial conditions are shown. The difference is seen to grow at an exponential rate of approximately 0.018. Comparable results were found for the L^∞ and L^1 norms. These tests provide experimental evidence that there presence of spatio-temporal chaos in the classical model (4)-(6).

Figure 4. Clearly, the balance is even more pronounced for multiple refuges and in higher dimensions.

We also improved the mathematical model by incorporating overcrowding effects, which also may be used as a control. We also examined the situation where a species may switch its primary food source based in regions of the domain, that is, a prey may switch to a predator, hence their roles are reversed. These models scenarios where influences on the landscape provide a competitive advantage to certain species. Both, role-reversal and overcrowding act as damping mechanisms and also may prevent blow-up in the invasive population. In particular, smaller refuge sizes in conjunction with role-reversal and overcrowding are required to prevent blow up. Of course, how does one enforce overcrowding in an ecosystem such that we obtain this desired effect? Can one devise mechanisms to facilitate this dispersal of population? We suggest one approach. Suppose we create a lure, such as a pheromone trap, that is placed in the refuge. This would lure the invasive species into the patch, where its growth would be controlled. Of course, the species would eventually exit the refuge in search for a higher concentration of food. Hence, in the future we plan to include spatially dependent diffusion constants to model this situation.

In our mathematical models we confirmed spatio-temporal chaos. We also see that overcrowding can effect the sorts of Turing patterns that might form. Since, environmental effects are inherently stochastic, part of our future investigations introduces stochasticity into the model. It is not known what effect this will have on the spatio-temporal chaos or Turing patterns that may emerge.

It is clear that our new mathematical modeling constructs and results are useful analytical and numerical tool for scientists interested in control of invasive species. Moreover, the results motivate and encourage numerous avenues of future exploration, many of which are currently under study and will be presented in future papers.

8. ACKNOWLEDGEMENT

We would like to acknowledge very helpful conversations with professor Pavol Quittner, professor Philippe Souplet and professor Joseph Shomberg, as pertains to the analysis of indefinite parabolic problems, as well as finite time blow-up in the superlinear parabolic problem, under various boundary conditions, and initial data restrictions.

REFERENCES

- [1] Arim, M., Abades, S., Neill, P., Lima, M., and Marquet, P., *Spread Dynamics of invasive species*, Proceedings of the National Academy of Sciences, 103(2), 374–378, 2006.
- [2] Averill, I. and Lou, Y., *On several conjectures from evolution of dispersal*, Journal of Biological Dynamics, vol.6, no.2, 117-130, 2012.
- [3] Aziz-Alaoui, M. A., *Study of a Leslie-Gower type tri-trophic population model*, Chaos, Solitons & Fractals, 14(8), 1275-1293, 2002.
- [4] Bampfylde, C.J. and Lewis, M.A., *Biological control through intraguild predation: case studies in pest control, invasive species and range expansion*, Bulletin of Mathematical Biology, 69, 1031-1066, 2007.
- [5] Beauregard, M. A. and Sheng, Q., *Solving degenerate quenching-combustion equations by an adaptive splitting method on evolving grids*, Comput. Struct., 122, 33-43, 2013.
- [6] Berryman, A., *The theory and classification of outbreaks*, Insect Outbreaks, pp 3-30, Academic Press, San Diego, CA, 1987.
- [7] Bryan, M.B.; Zalinski, D.; Filcek, K.B.; Libants, S.; Li, W.; Scribner, K.T., *Patterns of invasion and colonization of the sea lamprey in North America as revealed by microsatellite genotypes*, Molecular Ecology, 14(12), 3757-3773, 2005.

- [8] Canuto, C. and Quarteroni, A., *Approximation Results for Orthogonal Polynomials in Sobolev Spaces*, Mathematics of Computation, 38(157), 67–86, 1982.
- [9] Chen L. and Jungel, A., *Analysis of a parabolic cross-diffusion population model without self-diffusion*, J Diff Eq, 224(11), 39–59, 2006.
- [10] Clark, J.S., Lewis, M., and Horvath, L., *Invasion by extremes: Population spread with variation in dispersal and reproduction*, The American Naturalist, 157(5), 2001.
- [11] Cai, D., McLaughlin, D. and Shatah, J., *Spatiotemporal chaos in spatially extended systems*, Mathematics and Computers in Simulation, 55, 329–340, 2001.
- [12] Choh, Y., J.S., Sabelis, M., and Janssen, A. *Predator-prey role reversals, juvenile experience and adult antipredator behaviour*, Scientific Reports, 2(728), 1–6, 2012.
- [13] Don, W. and Solomonoff, A., *Accuracy and Speed in Computing the Chebyshev Collocation Derivative*, SIAM J Sci Comp, 16(6), 1253–1268, 1995.
- [14] Driesche, R.V. and Bellows, T., *Biological Control*, Kluwer Academic Publishers, Massachusetts, 1996.
- [15] Finke, D. and Denno, R. *Spatial refuge from intraguild predation: implications for prey suppression and trophic cascades*, Oecologia, 149, 265–275, 2006.
- [16] Follet, P. and Duan, J. *Nontarget Effects of Biological Control*, Dortrecht/Boston/London, Kluwer Academic Publishers, 2000.
- [17] Friedman, A., *Partial Differential Equations of Parabolic Type*, Prentice Hall Englewood Cliffs. N. J. 1964.
- [18] Gakkhar, S. and Singh, B., *Complex dynamic behavior in a food web consisting of two preys and a predator*, Chaos Solitons and Fractals, 24, 789–801, 2005.
- [19] Gomez-Lopez, J., *Global existence versus blow-up in superlinear indefinite parabolic problems*, Scientiae Mathematicae Japonicae Online, 449–472, 2004.
- [20] Gomez-Lopez, J. and Molina-Meyer, Marcela., *In the blink of an eye*, Progress in Nonlinear Differential Equations and Their Applications, 64, 291–327, 2005.
- [21] Gomez-Lopez, J. and Quittner, P., *Complete and Energy blow-up in indefinite superlinear parabolic problems*, Discrete & Continuous Dynamical Systems A, 14, 169–186, 2006.
- [22] White, K. A. J. and Gilligan, C.A., *Spatial heterogeneity in three species, plant-parasite-hyperparasite, systems*, Philosophical Transactions of the Royal Society of London. Series B: Biological Sciences 353.1368 (1998): 543–557.
- [23] Gottlieb, D. and Lustman, L., *The Spectrum of the Chebychev Collocation Operator for the Heat Equation*, SIAM J Num Anal, 20(5), 909–921, 1983.
- [24] Henry, D., *Geometric Theory of Semi-linear Parabolic Equations*, Lecture Notes in Mathematics 840, Springer-Verlag, New-York, 1984.
- [25] Hesthaven, J.; Gottlieb, S.; D. Gottlieb, D., *Spectral methods for time-dependent problems*, Cambridge University Press, New York, 2007.
- [26] Hillen, T.; Painter, K., *A users guide to PDE models for chemotaxis*, Journal of Mathematical Biology, 57, 183–217, 2009.
- [27] Chen, L. and Jungel, A., *Analysis of a parabolic cross-diffusion population model without self-diffusion*, Journal of Differential Equations, Vol. 224, number 11, 39–59, 2006.
- [28] Chen, L. and Jungel, A., *Analysis of a multi-dimensional parabolic population model with strong cross-diffusion*, SIAM Journal of Mathematical Analysis, Vol. 36, 301–322, 2004.
- [29] Kar, T.K., *Stability analysis of a prey-predator model incorporating a prey refuge*, Communications in Nonlinear Science and Numerical Simulation, 10, 681–691, 2004.
- [30] Hood, J., *Asian carp: State’s fish kill in Chicago Sanitary and Ship Canal yield only 1 Asian carp*, www.articles.chicagotribune.com.
- [31] Medvinsky, A., Petrovskii, S., Tikhonova, I., Malchow, H. and Li, B., *Spatiotemporal Complexity of Plankton and Fish Dynamics*, SIAM Reveiw, 44(3), 311–370, 2002.
- [32] Kumari, N., *Pattern Formation in Spatially Extended Tritrophic Food Chain Model Systems: Generalist versus Specialist Top Predator*, ISRN Biomathematics, Volume 2013 (2013), Article ID 198185.
- [33] Letellier, C. and Aziz-Alaoui, M. A., *Analysis of the dynamics of a realistic ecological model*, Chaos, Solitons & Fractals, 13, 95–107, 2002.
- [34] Loda, S.M., Pemberton, R.W., Johnson, M.T. and Follet, P.A. *Nontarget effects-The Achilles heel of biological control? Retrospective Analyses to reduce risk associated with biocontrol introductions.*, Annual Reveiw of Entomology, 48, 365–396, 2003.

- [35] Lou, Y.; Munther, D., *Dynamics of a three species competition model*, Discrete & Continuous Dynamical Systems-A, 32, 3099-3131, 2012.
- [36] Ludwig, D., Jones, D., and Holling, C., *Qualitative analysis of insect outbreak systems: The spruce budworm and forest* The journal of animal ecology, vol. 47, no.1, 315-332, 1978.
- [37] Morgan, R., *GMRES with Deflated Restarting*, SIAM J Sci Comput, 24, 20-37, 2002.
- [38] Myers, J.H.; Simberloff, D; Kuris, A. M.; Carey, J.R., *Eradication revisited: dealing with exotic species*, Trends in Ecology & Evolution, 15, 316-320, 2000.
- [39] New York Sea Grant. Policy Issues. *Zebra Mussel Clearinghouse Information Review*, 5(3), 6-7, 1994.
- [40] Okubo, A.; Maini, P.K.; Williamson, M.H.; Murray, J.D., *On the Spatial Spread of the grey squirrel in Britain*, Proceedings of the Royal Society of London, Series B, 238, 113-125, 1989.
- [41] Parshad, R.D. and Upadhyay, R. K., *Investigation of long time dynamics of a diffusive three species aquatic model*, Dynamics of Partial Differential Equations, 7(3), 217-244, 2010.
- [42] Parshad, R.D. , Abderrahmanne, H., Upadhyay, R. K. and Kumari, N., *Finite time blowup in a realistic food chain model*, ISRN Biomathematics, Volume 2013 (2013), Article ID 424062.
- [43] Parshad, R. D., Kumari, N., Kasimov, A. R., Abderrahmane, H. A., *Turing Patterns and long time behavior in a three-species model*, Mathematical Biosciences, 254, 83-102, 2014.
- [44] Parshad, R. D., Kumari, N. and Kouachi, S., *A remark on "Study of a Leslie-Gower-type tritrophic population model [Chaos, Solitons and Fractals 14 (2002) 1275-1293]*, Chaos, Solitons & Fractals, 71(2), 22-28, 2015.
- [45] Pazy, A.S., *Semigroups of Linear Operators and Applications to Partial Differential Equations*, Applied Math. Sciences 44, Springer-Verlag, New York, 1983.
- [46] Philips, B.; Shine, R., *Adapting to an invasive species: Toxic cane toads induce morphological change in Australian snakes*, Proceedings of National Academy of Sciences USA, 101(49), 17150-17155, 2004.
- [47] Pimentel, D.; Zuniga, R.; Morrison, D., *Update on the environmental and economic costs associated with alien-invasive species in the united states*, Ecological Economics, 52(3), 273-288, 2005.
- [48] Quittner, P. and Souplet, P. *Superlinear Parabolic Problems: Blow-up, Global Existence and Steady States*, Birkhauser Verlag, Basel, 2007.
- [49] Ackermann, N., Bartsch, T., Kaplicky, P and Quittner, P. *A Priori Bounds, Nodal Equilibria and Connecting Orbits in Indefinite Superlinear Parabolic Problems*, Transactions of the American Mathematical Society, 360(7), 3493-3539, 2008.
- [50] Rodda, G.H.; Jarnevich, C.S.; Reed, R.N., *What parts of the US mainland are climatically suitable for invasive alien pythons spreading from everglades national park?*, Molecular Ecology, 14(12), 3757-3773, 2005.
- [51] Rothe, F., *Global Solutions of Reaction-Diffusion Systems*, Lecture Notes in Math. 1072, Springer-Verlag, Berlin, 1984.
- [52] Shen, J., *Efficient Spectral-Galerkin Method II. Direct Solvers of Second- and Fourth-Order Equations Using Chebyshev Polynomials*, SIAM J Sci Comp, 16(1), 74-87, 1995.
- [53] Shigesada N. and K. Kawasaki, "Biological invasions: Theory and practice," Oxford University Press, Oxford, 1997.
- [54] Simberloff, D., *Introduced species: The threat to biodiversity and what can be done*, <http://www.actionbioscience.org/biodiversity/simberloff.html> .
- [55] Smith, James G and Phillips, Ben L. *Toxic Tucker: The Potential Impact of Cane Toads on Australian Reptiles*, Pacific Conservation Biology, 12(1), 2006: [40]-49.
- [56] Sun, G., Zhang, G., Jin, Z. and Li, L., *Predator cannibalism can give rise to regular spatial pattern in a predator-prey system*, Nonlinear Dynamics, vol 58, no.1-2, 75-84, 2009.
- [57] Smoller, J., *Shock Waves and Reaction-Diffusion Equations*, Springer-Verlag, New York, 1983.
- [58] Straughan, B. *Explosive Instabilities in Mechanics*, Springer-Verlag, Heidelberg, 1998.
- [59] Strikwerda, J.C., *Finite Difference Schemes and Partial Differential Equations, 2nd Edition*, SIAM, 172-185, 2004.
- [60] Upadhyay, R. K., Iyengar, S.R.K. and Rai, V., *Chaos: an ecological reality?*, International Journal of Bifurcations and Chaos, 8, 1325-1333, 1998.
- [61] Upadhyay, R. K. and Rai, V., *Why chaos is rarely observed in natural populations?*, Chaos, Solitons & Fractals, 8(12), 1933-1939, 1997.

- [62] Upadhyay, R.K., Iyengar, S.R.K., and Rai, V. *Stability and complexity in ecological systems*, Chaos, Solitons & Fractals, 11, 533-542, 2000.
- [63] Upadhyay, R. K., Naji, R. K., Kumari, N., *Dynamical complexity in some ecological models: effects of toxin production by phytoplanktons*, Nonlinear analysis: Modeling and Control, 12(1), 123-138, 2007.
- [64] Upadhyay, R. K. and Iyengar, S.R.K., *Effect of seasonality on the dynamics of 2 and 3 species prey-predator systems*, Nonlinear Analysis: Real World Applications, 6, 509-530, 2005.
- [65] Van Driesche, R. and Bellows, T. "Biological Control", Kluwer Academic Publishers, Massachusetts, 1996.
- [66] Wittmeier, B., *Mathematical Biologist applies hard data to soft science* Edmonton Journal, 2012.
- [67] Z. Xie, *Cross diffusion induced Turing instability for a three species food chain model*, Journal of Mathematical Analysis and Applications, vol 388, no.1, 539-547, 2012.
- [68] Songmu Zheng, *Nonlinear evolution equations*, Monographs and Surveys in Pure and Applied Mathematics - Volume 133, Chapman & Hall/CRC, Boca Raton, 2004.

E-mail address: rparshad@clarkson.edu

E-mail address: kblack@clarkson.edu

E-mail address: quansaek@clarkson.edu

E-mail address: beauregama@sfasu.edu